ARTICLE

doi:10.1038/nature23876

Ascorbate regulates haematopoietic stem cell function and leukaemogenesis

Michalis Agathocleous[1], Corbin E. Meacham[1], Rebecca J. Burgess[1], Elena Piskounova[1], Zhiyu Zhao[1], Genevieve M. Crane[1], Brianna L. Cowin[1], Emily Bruner[1], Malea M. Murphy[1], Weina Chen[2], Gerald J. Spangrude[3], Zeping Hu[1], Ralph J. DeBerardinis[1,4] & Sean J. Morrison[1,4]

Stem–cell fate can be influenced by metabolite levels in culture, but it is not known whether physiological variations in metabolite levels in normal tissues regulate stem–cell function *in vivo*. Here we describe a metabolomics method for the analysis of rare cell populations isolated directly from tissues and use it to compare mouse haematopoietic stem cells (HSCs) to restricted haematopoietic progenitors. Each haematopoietic cell type had a distinct metabolic signature. Human and mouse HSCs had unusually high levels of ascorbate, which decreased with differentiation. Systemic ascorbate depletion in mice increased HSC frequency and function, in part by reducing the function of Tet2, a dioxygenase tumour suppressor. Ascorbate depletion cooperated with *Flt3* internal tandem duplication (*Flt3*^{ITD}) leukaemic mutations to accelerate leukaemogenesis, through cell–autonomous and possibly non–cell–autonomous mechanisms, in a manner that was reversed by dietary ascorbate. Ascorbate acted cell–autonomously to negatively regulate HSC function and myelopoiesis through Tet2–dependent and Tet2–independent mechanisms. Ascorbate therefore accumulates within HSCs to promote Tet activity *in vivo*, limiting HSC frequency and suppressing leukaemogenesis.

A fundamental question is whether physiological variations in metabolite levels influence stem-cell fate, tissue homeostasis and tumour suppression. Genetic changes in metabolic enzymes can alter stem-cell function[1] and cause oncogenic transformation[2]. Dietary changes alter stem-cell function in multiple systems by regulating signalling, for example by insulin and/or IGF[3]. It is generally unknown whether dietary changes alter stem-cell function by changing metabolite levels; however, muscle stem-cell ageing is regulated by changes in NAD^+ levels[4]. Differentiation *in vivo* is accompanied by metabolic changes[5], and experimental manipulation of metabolite levels in culture can modulate pluripotent stem-cell differentiation[6–8]. However, it is unclear whether physiological variation in metabolite levels influences stem-cell fate *in vivo*.

Studies of stem-cell metabolism have been limited by the fact that metabolomics is typically performed using millions of cells and it is generally impossible to isolate that many stem cells directly from tissues. Metabolomics has been performed on haematopoietic stem/progenitor cells either by isolating large numbers of heterogeneous Lineage$^-$Sca-1$^+$Kit$^+$ (LSK) cells[9] or by pooling HSCs from 120 mice to perform a single experiment[10]. Others have studied stem-cell metabolism by characterizing the phenotypes of knockout mice or metabolism in culture[11]. However, it has been difficult to routinely compare metabolite levels within rare cell populations in tissues. To address this we have optimized the sensitivity of metabolomics.

Metabolomics in rare cell populations

We performed metabolomics in rare cell populations by combining rapid cell isolation by flow cytometry with liquid chromatography–mass spectrometry (Extended Data Fig. 1a). Cells were kept cold during cell purification and the levels of most metabolites remained stable during cell purification (Extended Data Fig. 1b–f). We detected approximately 60 metabolites, covering a range of metabolic pathways, from 10,000 HSCs (Extended Data Fig. 2a).

We compared CD150$^+$CD48$^-$LSK HSCs and CD150$^-$CD48$^-$LSK multipotent progenitors (MPPs) to a variety of restricted haematopoietic progenitors isolated from mouse bone marrow (Fig. 1a). HSCs and MPPs did not differ in the metabolites that we measured (Extended Data Fig. 2b), but did differ from all restricted progenitor populations (Fig. 1a). Almost all of the metabolites that we detected had distinct enrichment patterns for different cell types (Extended Data Fig. 2c, d). Therefore, even linearly related cells within a similar *in vivo* environment exhibit metabolic differences.

One of the most enriched metabolites in HSCs and MPPs was ascorbate (vitamin C) (Extended Data Fig. 2c). Ascorbate remained stable during cell purification (Extended Data Fig. 1g). Ascorbate levels were 2- to 20-fold higher in the mixed population of HSCs and MPPs (hereafter HSCs/MPPs) compared to other haematopoietic progenitors, and decreased with differentiation (Fig. 1b).

Ascorbate regulates HSC frequency

Humans obtain ascorbate exclusively through their diet, but mice and most other mammals synthesize ascorbate in the liver using the enzyme gulonolactone oxidase (*Gulo*)[12]. Ascorbate is taken up by most cells through two dedicated transporters encoded by *Slc23a1* and *Slc23a2* (ref. 12). *Slc23a2* was expressed by most haematopoietic cells, but at 14-fold higher levels in HSCs/MPPs compared to restricted haematopoietic progenitors (Fig. 1c). *Slc23a2* expression, similar to ascorbate levels, decreased with differentiation (Fig. 1c). Ascorbate levels in haematopoietic cells correlated strongly with *Slc23a2* expression ($R^2 = 0.94$) (Extended Data Fig. 3a). *Slc23a1* and *Gulo* are not expressed by haematopoietic cells[13]. Therefore, ascorbate accumulation in HSCs was probably due to high *Slc23a2* expression.

To test whether ascorbate regulates HSC function we analysed *Gulo*$^{-/-}$ mice, which are unable to synthesize ascorbate and, like humans, obtain ascorbate exclusively through their diet. *Gulo*$^{-/-}$ mice, born to *Gulo*$^{+/-}$ females, were developmentally normal and received

[1]Children's Research Institute and the Department of Pediatrics, University of Texas Southwestern Medical Center, Dallas, Texas 75390, USA. [2]Department of Pathology, University of Texas Southwestern Medical Center, Dallas, Texas 75390, USA. [3]Department of Medicine, University of Utah, Salt Lake City, Utah, USA. [4]Howard Hughes Medical Institute, University of Texas Southwestern Medical Center, Dallas, Texas 75390, USA.

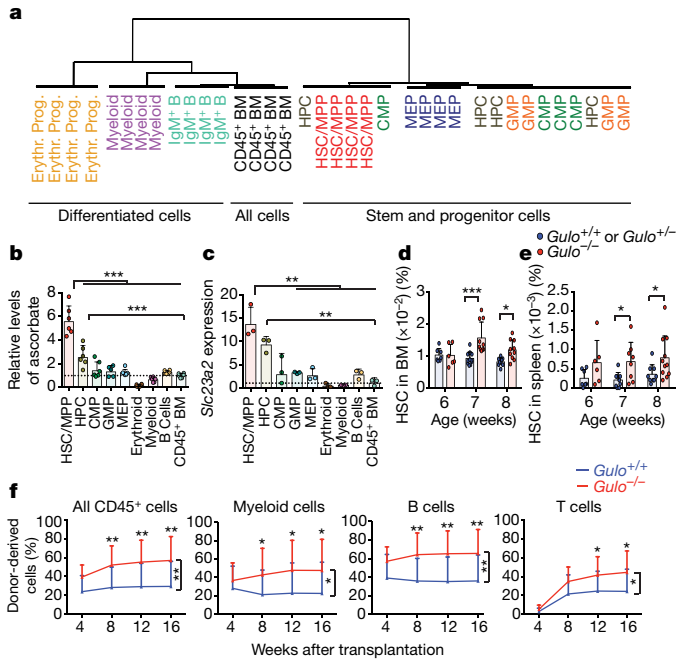

Figure 1 | HSCs have high ascorbate levels and ascorbate depletion increases HSC frequency. a, Unsupervised clustering of metabolomic data from haematopoietic stem and progenitor cell populations (see Methods for the markers used to isolate each population; one experiment representative of a total of four experiments). BM, bone marrow; CMP, common myeloid progenitor; Erythr. prog., erythroid progenitor; GMP, granulocyte–macrophage progenitor; IgM^+ B, IgM^+ B cell; MEP, megakaryocyte–erythroid progenitor. **b**, **c**, Ascorbate and *Slc23a2* expression levels relative to $CD45^+$ bone marrow cells (**b**, $n = 6$ mice from two independent experiments. **c**, $n = 3$ mice from two independent experiments). **d**, **e**, HSC frequencies in $Gulo^{-/-}$ ascorbate-depleted and littermate-control mice at 6, 7 or 8 weeks of age ($n = 6$–11 mice per genotype per time point, 3–6 independent experiments per time point). **f**, Percentage of donor-derived haematopoietic cells after competitive transplantation of 500,000 donor $Gulo^{+/+}$ or $Gulo^{-/-}$ bone marrow cells along with 500,000 competing wild-type recipient cells into irradiated recipient mice (a total of three donors and 14–15 recipients per genotype for three independent experiments). The exact number of mice analysed and the values obtained for each mouse are provided in the Source Data. Statistical significance was assessed with *t*-tests (**b**, **c**) or two-way ANOVAs followed by Fisher's least significant difference (LSD) tests for individual time points (**d**–**f**). All data represent mean ± s.d. We corrected for multiple comparisons by controlling the false discovery rate. $*P < 0.05$, $**P < 0.01$, $***P < 0.001$.

ascorbate from their mothers until they were weaned at four weeks of age. They subsequently became ascorbate depleted when maintained on a standard mouse diet, which contains very little ascorbate. By 6–8 weeks of age, $Gulo^{-/-}$ mice were smaller than $Gulo^{+/+}$ or $Gulo^{+/-}$ littermates and had fewer bone marrow and spleen cells (Extended Data Fig. 3b–d). In the bone marrow and spleen of $Gulo^{-/-}$ mice, HSC frequency (Fig. 1d, e) and HSC number normalized to body mass (Extended Data Fig. 3e, f) were significantly higher than in littermate controls at 7 and 8 weeks of age. The frequencies of most of the other haematopoietic progenitors, and their rates of cell division, did not significantly differ between $Gulo^{-/-}$ and control mice (Extended Data Fig. 3g–t). $Gulo^{-/-}$ thymuses were hypocellular (Extended Data Fig. 3u), consistent with a known requirement for ascorbate in thymocyte maturation[14].

Upon competitive transplantation into irradiated mice, $Gulo^{-/-}$ bone marrow cells showed significantly higher levels of reconstitution of cells in all lineages compared to control cells (Fig. 1f). Therefore, HSC frequency was significantly higher in ascorbate-depleted mice.

Ascorbate regulates the function of Tet in HSCs

Ascorbate is a cofactor for several α-ketoglutarate-dependent dioxygenases[15], including Jumonji histone demethylases[16]. However, ascorbate depletion did not significantly increase the levels of several histone methylation marks (Extended Data Fig. 4a). Although ascorbate promotes the activity of prolyl 4-hydroxylase during collagen synthesis[17], we did not detect a pronounced loss of bone collagen in ascorbate-depleted mice (Extended Data Fig. 4b). Nevertheless, a loss of collagen, or collagen organization, may be observed with longer-term ascorbate depletion. Ascorbate can regulate hydroxylase enzymes during carnitine biosynthesis in culture[18]; however, we did not detect any effect of ascorbate depletion on carnitine or acetylcarnitine levels in haematopoietic cells (Extended Data Fig. 4c). We also did not detect any effect of ascorbate depletion on levels of reactive oxygen species in haematopoietic cells (Extended Data Fig. 4d). Ascorbate can act as a cofactor for prolyl hydroxylases that degrade hypoxia inducible factors (HIFs)[19], but HIF-1α and HIF-2α are not required for HSC function[20]. Despite our inability to detect an effect of ascorbate depletion on the function of these enzymes, they could potentially contribute to the effects of ascorbate depletion on HSCs.

Ascorbate promotes the activity of Tet enzymes in culture[7,21–23], although it remains unclear whether ascorbate limits Tet function *in vivo*. Tet enzymes convert 5-methylcytosine (5mC) to 5-hydroxymethylcytosine (5hmC), and subsequently catalyse some of the steps towards unmethylated cytosine[24,25]. Mutations that inactivate *Tet2* are early events in leukaemogenesis[26] that increase HSC frequency and self-renewal[27–29] and cause leukaemia when combined with other mutations[30–32]. Consistent with previous studies[27–29], conditional deletion of *Tet2* in adult haematopoietic cells significantly increased HSC frequency and function (Extended Data Fig. 5a–h), similar to what was observed after ascorbate depletion.

To analyse whether physiological variations in ascorbate regulate Tet function in haematopoietic cells, we sustained $Gulo^{-/-}$ mice with low levels of ascorbate in the drinking water for 3–6 months. These mice showed approximately tenfold lower levels of ascorbate in the plasma and in haematopoietic cells relative to littermate controls (Fig. 2c and Extended Data Figs 4e, 6e, f). Ascorbate levels in $Gulo^{-/-}$ mice were therefore similar to those observed in 5% of people in western countries[33]. Ascorbate-depleted $Gulo^{-/-}$ mice had significantly reduced 5hmC levels in HSCs/MPPs, haematopoietic progenitor cells (HPCs), myeloid progenitors and unfractionated bone marrow cells relative to littermate controls (Fig. 2a), but they had normal 5mC levels, suggesting that these cells had reduced Tet activity (Fig. 2b). Similar to ascorbate, 5hmC levels were highest in HSCs/MPPs and these levels decreased with differentiation (Fig. 2a).

To investigate whether ascorbate regulates 5hmC levels by modulating Tet2 activity, we compared 5hmC levels in haematopoietic cells from $Gulo^{-/-}$ mice, in *Tet2*-deficient haematopoietic cells ($Tet2^{\Delta/\Delta}$) and in $Gulo^{-/-}$;$Tet2^{\Delta/\Delta}$ compound mutant haematopoietic cells. *Gulo* deficiency and *Tet2* deficiency each significantly reduced 5hmC levels in all cell populations relative to wild-type controls, but HSCs/MPPs and HPCs from $Gulo^{-/-}$;$Tet2^{\Delta/\Delta}$ compound mutant mice did not have significantly lower 5hmC levels compared to the same cells from $Tet2^{\Delta/\Delta}$ mice (Fig. 2a). Therefore, most of the effect of ascorbate depletion on 5hmC levels in HSCs/MPPs and HPCs was mediated by changes in the function of Tet2. Myeloid progenitors did have significantly lower 5hmC levels in $Gulo^{-/-}$;$Tet2^{\Delta/\Delta}$ compound mutant mice compared to $Tet2^{\Delta/\Delta}$ mice (Fig. 2a). Ascorbate depletion, therefore, reduced 5hmC levels in myeloid progenitors through Tet2-dependent and Tet2-independent mechanisms. The Tet2-independent mechanisms may include effects on the function of Tet1 or Tet3 (Fig. 2a).

To investigate whether Tet2 mediates the effects of ascorbate depletion on HSC function, we competitively transplanted donor *Mx1-Cre*;$Tet2^{fl/fl}$ and wild-type bone marrow cells into wild-type or ascorbate-depleted $Gulo^{-/-}$ recipient mice and treated the mice with polyinosinic:polycytidylic acid (poly(I:C)) to delete *Tet2* six weeks

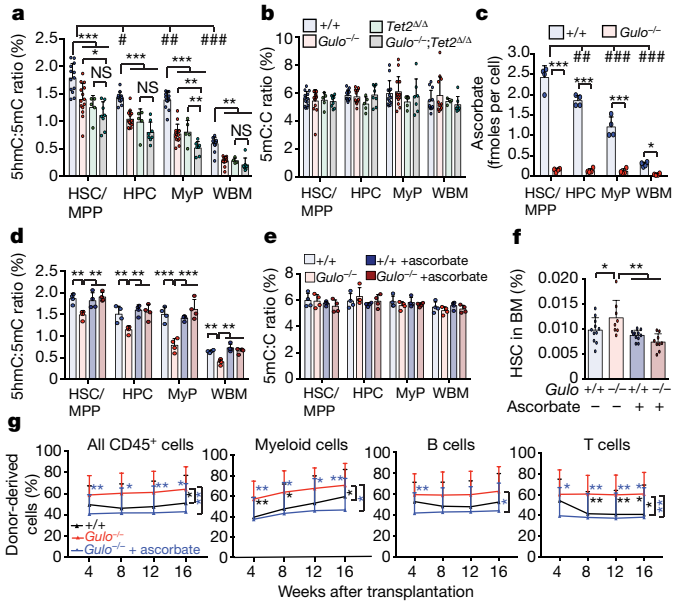

Figure 2 | Ascorbate depletion reduces Tet2 activity in HSCs and progenitors in *vivo*. **a**, **b**, 5hmC:5mC and 5mC:cytosine (C) ratios in sorted cell populations from 4–6-month-old wild-type ($n = 13$ mice), *Gulo*$^{-/-}$ ($n = 14$ mice), *Tet2*$^{\Delta/\Delta}$ ($n = 5$ mice) and *Tet2*$^{\Delta/\Delta}$;*Gulo*$^{-/-}$ ($n = 8$ mice) mice from 10 independent experiments. *Comparisons between genotypes and #comparisons between cell types; $\#P < 0.05$, $\#\#P < 0.01$, $\#\#\#P < 0.001$; $*P < 0.05$, $**P < 0.01$, $***P < 0.001$. **c**, Ascorbate levels in cells from four-month-old mice (a total of $n = 4$ mice per condition from two independent experiments). **d**, **e**, 5hmC:5mC and 5mC:C ratios in sorted cell populations from four-month-old mice with or without ascorbate feeding (a total of $n = 4$ mice per condition from three independent experiments). **f**, HSC frequency in eight-week-old mice (a total of $n = 8$–11 mice per genotype from six independent experiments). **g**, Percentage of donor-derived haematopoietic cells after competitive transplantation of 500,000 donor bone marrow cells from *Gulo*$^{+/+}$ or *Gulo*$^{-/-}$ mice, or *Gulo*$^{-/-}$ mice supplemented with ascorbate, along with 500,000 competitor wild-type cells in irradiated recipient mice (a total of four donors and 19–20 recipients per genotype from four independent experiments). Statistical significance was assessed with one-way (**a**, **b**, **d**–**f**) or two-way (**c**) ANOVAs, Kruskal–Wallis tests (for abnormally distributed data in **a**, **b**), or with a non-parametric mixed model followed by Kruskal–Wallis tests for individual time points (**g**). All data represent mean ± s.d. We corrected for multiple comparisons by controlling the false discovery rate. $*P < 0.05$, $**P < 0.01$, $***P < 0.001$.

after transplantation (Extended Data Fig. 6a, c, d). *Tet2*-deficient HSCs transplanted into wild-type recipients gave significantly higher levels of reconstitution than wild-type HSCs, as expected, but this effect was attenuated in ascorbate-depleted *Gulo*$^{-/-}$ recipients (Extended Data Fig. 6d). The increase in HSC function by ascorbate depletion is, therefore, mediated in part by Tet2, because ascorbate depletion increased cell reconstitution more from the wild-type competitor cells than from *Tet2*-deficient HSCs.

Supplementation with higher levels of dietary ascorbate (ascorbate repletion) increased ascorbate levels in *Gulo*$^{-/-}$ mice to those observed in wild-type mice (Extended Data Fig. 6e, f). This prevented the decrease in 5hmC levels in HSCs and restricted progenitors (Fig. 2d, e) as well as the increase in HSC frequency and function (Fig. 2f, g). Therefore, these phenotypes are caused by ascorbate depletion.

Addition of ascorbate to cultured HSCs significantly reduced monocytic differentiation and promoted erythroid differentiation (Extended Data Fig. 6g–m). This is consistent with the conclusion that ascorbate promotes Tet2 function, because *Tet2* deficiency promotes monocytic differentiation and reduces erythroid differentiation in culture[28,34].

We performed RNA-sequencing analysis in HSCs/MPPs from *Gulo*$^{-/-}$, *Tet2*$^{\Delta/\Delta}$, *Gulo*$^{-/-}$;*Tet2*$^{\Delta/\Delta}$ and control mice and found that some of the changes in gene expression in ascorbate-depleted HSCs/MPPs were also observed in *Tet2*-deficient HSCs/MPPs (Extended Data Fig. 7). The number of transcripts in *Gulo*$^{-/-}$ and *Tet2*$^{\Delta/\Delta}$ HSCs/MPPs that changed in the same direction relative to control HSCs/MPPs was significantly higher than expected by chance and included regulators of haematopoiesis, cell death and differentiation (Extended Data Fig. 7b). A common group of gene sets were downregulated in both *Gulo*$^{-/-}$ and *Tet2*$^{\Delta/\Delta}$ HSCs/MPPs (Extended Data Fig. 7c).

Ascorbate depletion cooperates with Flt3(ITD)

TET2 mutations cooperate with *FLT3*^{ITD} mutations to cause acute myeloid leukaemia (AML)[31,35]. Consistent with this, *Tet2* deficiency and *Flt3*^{ITD} mutations cooperated to significantly increase the frequencies of HPCs and some of the myeloid progenitors (Extended Data Fig. 8a–f) and to increase myelopoiesis compared to *Tet2* deficiency or *Flt3*^{ITD} mutations alone in competitive reconstitution assays (Extended Data Fig. 8g).

To investigate whether ascorbate depletion cooperates with *Flt3*^{ITD} mutations, we transplanted *Flt3*^{ITD} or control bone marrow cells along with wild-type competitors into irradiated recipients that were either ascorbate-replete wild-type mice or ascorbate-depleted *Gulo*$^{-/-}$ mice. *Flt3*^{ITD} donor cells had significantly higher levels of myeloid cell reconstitution (Fig. 3a) as well as MPPs, HPCs and myeloid progenitors in the bone marrow (Fig. 3b) in ascorbate-depleted compared to wild-type recipients. Consistent with the observation that *Flt3*^{ITD} and *Tet2* deficiency particularly increase the frequency of CD48^{+}LSK HPC cells[31], the frequency of *Flt3*^{ITD} donor HPCs was significantly increased in the bone marrow and spleen of ascorbate-depleted *Gulo*$^{-/-}$ recipients relative to wild-type recipients (Fig. 3c, d). Ascorbate depletion therefore cooperates with *Flt3*^{ITD} to promote myelopoiesis in a manner similar to reduced Tet2 function.

To test whether ascorbate depletion increases the competitiveness of *Flt3*^{ITD} stem and progenitor cells in part by reducing Tet2 function, we competitively transplanted *Flt3*^{ITD};*Tet2*$^{\Delta/\Delta}$ bone marrow cells into wild-type and *Gulo*$^{-/-}$ mice. Unlike *Flt3*^{ITD} cells (Fig. 3a), *Flt3*^{ITD};*Tet2*$^{\Delta/\Delta}$ cells did not give rise to higher numbers of donor myeloid cells in ascorbate-depleted relative to ascorbate-replete mice (Fig. 3e). Indeed, *Flt3*^{ITD};*Tet2*$^{\Delta/\Delta}$ cells tended to have lower levels of myelopoiesis in ascorbate-depleted compared to control recipients, potentially reflecting increased myelopoiesis by wild-type competitor cells in the ascorbate-depleted mice. Because *Tet2* deficiency eliminated the competitive advantage conferred by ascorbate depletion in *Flt3*^{ITD} cells, ascorbate depletion promoted myelopoiesis mainly by reducing Tet2 function.

Flt3^{ITD} cells produced significantly more B cells in ascorbate-depleted compared to wild-type recipients (Fig. 3a). Because *Tet2* deficiency did not increase B cell lymphopoiesis by *Flt3*^{ITD} cells (Extended Data Fig. 8g), this suggests that ascorbate depletion promoted B cell lymphopoiesis through Tet2-independent mechanisms, potentially through reduced Tet1 function, which regulates B cell lymphopoiesis[36]. Consistent with this possibility, *Flt3*^{ITD};*Tet2*$^{\Delta/\Delta}$ cells tended to generate more B cells in ascorbate-depleted compared to wild-type recipients (Fig. 3e).

We investigated whether ascorbate repletion can reverse the increase in *Flt3*^{ITD}-driven myelopoiesis caused by ascorbate depletion. We transplanted *Flt3*^{ITD} cells from ascorbate-depleted *Gulo*$^{-/-}$ recipients into secondary recipients that were either ascorbate depleted or ascorbate replete (Extended Data Fig. 8h). *Flt3*^{ITD}-driven myelopoiesis remained high in ascorbate-depleted recipients, but decreased in ascorbate-replete recipients, suggesting that the effects of ascorbate depletion on *Flt3*^{ITD}-driven myelopoiesis are reversible (Extended Data Fig. 8h).

To investigate whether ascorbate acts cell-autonomously to regulate HSC function, we competitively transplanted fetal liver haematopoietic cells from ascorbate transporter, *Slc23a2*-deficient mice or littermate controls, into wild-type mice with normal ascorbate levels (Fig. 3f). In this experiment, only the *Slc23a2*$^{-/-}$ donor cells were ascorbate

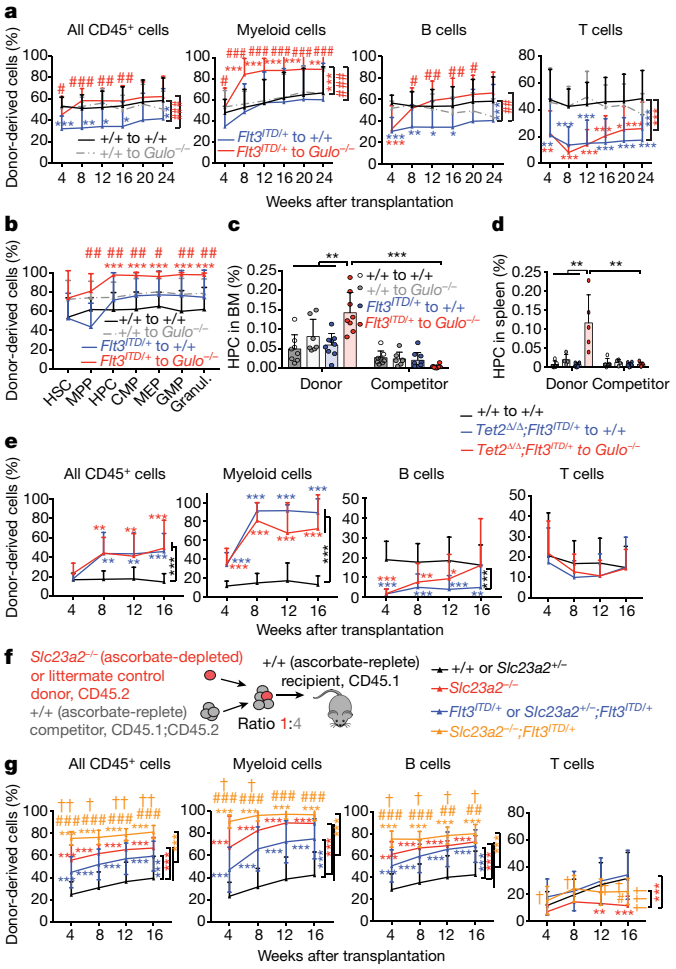

Figure 3 | Low ascorbate levels cooperate with *Flt3*^{ITD} to promote myelopoiesis, in part by reducing *Tet2* function, and cell-autonomously promote HSC function. a–d, Competitive transplantation of 500,000 donor bone marrow cells from *Flt3*$^{ITD/+}$ mice or littermate controls along with 500,000 competing wild-type cells into irradiated wild-type (ascorbate-replete) or *Gulo*$^{-/-}$ (ascorbate-depleted) recipient mice (a total of four donor mice and 13–20 recipient mice per treatment from two independent experiments). **a**, Donor cell reconstitution levels in the blood. **b**, The percentages of donor-derived cells in the bone marrow. **c**, **d**, Frequencies of donor- and competitor-derived CD48^{+}LSK HPC cells. **e**, Competitive transplantation of 500,000 donor bone marrow cells of the indicated genotypes along with 1,500,000 competitor wild-type cells in irradiated wild-type (ascorbate-replete) or *Gulo*$^{-/-}$ (ascorbate-depleted) mice (a total of four donor mice and 15 recipient mice per treatment from four independent experiments). **f**, **g**, Competitive transplantation of 500,000 donor fetal liver cells from the indicated genotypes along with 2,000,000 competing wild-type bone marrow cells in irradiated wild-type recipient mice (for *Slc23a2*$^{+/+}$ (+/+) and *Slc23a2*$^{+/-}$, 10 donor and 50 recipient mice; for *Slc23a2*$^{-/-}$, 4 donors and 20 recipients; for *Flt3*$^{ITD/+}$ and *Slc23a2*$^{+/-}$;*Flt3*$^{ITD/+}$, 6 donors and 30 recipients; for *Slc23a2*$^{-/-}$;*Flt3*$^{ITD/+}$, 5 donors and 24 recipients, from six independent experiments). *Slc23a2*$^{+/+}$ and *Slc23a2*$^{+/-}$ genotypes were pooled as they showed no statistically significant differences. **g**, Percentage of donor-derived haematopoietic cells. *Comparisons to wild-type mice (black line), #comparisons to *Flt3*$^{ITD/+}$ mice (blue line) and †comparisons to *Slc23a2*$^{-/-}$ mice (red line) at different time points or between lines as indicated by the brackets. All data represent mean ± s.d. Statistical significance was assessed with a non-parametric mixed model followed by Kruskal–Wallis tests for individual time points or cell types (**a**, **b**, **e**, **g**), one-way ANOVAs followed by Fisher's LSD tests (between genotypes in **c**, **d**) and Mann–Whitney *U*-tests (between donor and competitor in **c**, **d**). We corrected for multiple comparisons by controlling the false discovery rate. *$P < 0.05$, **$P < 0.01$, ***$P < 0.001$; #$P < 0.05$, ##$P < 0.01$, ###$P < 0.001$; †$P < 0.05$, ††$P < 0.01$, †††$P < 0.001$.

depleted while other cells in the recipient mice had normal ascorbate levels (Extended Data Fig. 8i). The *Slc23a2*$^{-/-}$ cells showed significantly higher levels of cell reconstitution compared to control cells in all lineages, except the T cell lineage (Fig. 3g). *Slc23a2*$^{-/-}$ cells also gave rise to higher levels of myelopoiesis compared to control cells (Extended Data Fig. 8j). The increased reconstitution from *Slc23a2*$^{-/-}$ cells reflected increased HSC function after transplantation, because the frequency of HSCs in donor fetal livers did not differ significantly between *Slc23a2*$^{-/-}$ and controls (Extended Data Fig. 8k). *Slc23a2*$^{-/-}$;*Flt3*^{ITD} cells also reconstituted blood cells at significantly higher levels compared to *Slc23a2*$^{-/-}$ cells, *Flt3*^{ITD} cells, or wild-type donor cells, and had increased myelopoiesis compared to *Flt3*^{ITD} or wild-type cells (Fig. 3g and Extended Data Fig. 8j). Therefore, ascorbate is taken up by haematopoietic stem and progenitor cells and then cell-autonomously regulates HSC function and *Flt3*^{ITD}-driven myelopoiesis.

Ascorbate suppresses leukaemogenesis

Reduced Tet2 (ref. 31), or Tet2 and Tet3 (ref. 37), function promotes AML development. We tested whether ascorbate depletion accelerates AML development from *Flt3*^{ITD};*Tet2*$^{Δ/+}$ cells by transplanting equal numbers of these cells into wild-type or *Gulo*$^{-/-}$ mice, leading to similar levels of donor cell engraftment (Extended Data Fig. 9a–c). Ascorbate-depleted recipients had significantly higher numbers of myeloblasts, white blood cells (WBCs), blood myeloid cells and spleen cells compared to wild-type recipients (Fig. 4a, c and Extended Data Fig. 9d–f). All ascorbate-depleted recipients died within 50 days of transplantation, whereas most wild-type recipients remained alive for at least 300 days after transplantation (Fig. 4b). CD48^{+}CD150^{-}LSK HPC cells, which can initiate AML from *Flt3*^{ITD};*Tet2*$^{Δ/+}$ cells[31], expanded to a significantly greater extent in the bone marrow (Extended Data Fig. 9g) and spleen (Fig. 4d) of ascorbate-depleted compared to wild-type recipients. Moribund ascorbate-depleted recipients had a spectrum of disease from myeloproliferative neoplasm to AML, whereas none of the control recipients met the criteria for AML. Therefore, ascorbate depletion accelerated the development of AML from *Flt3*^{ITD};*Tet2*$^{Δ/+}$ cells.

We subsequently investigated whether ascorbate depletion promotes leukaemogenesis through Tet2-independent mechanisms. We transplanted *Tet2*$^{Δ/+}$;*Flt3*^{ITD} and *Tet2*$^{Δ/Δ}$;*Flt3*^{ITD} cells into wild-type or ascorbate-depleted *Gulo*$^{-/-}$ recipients, then re-isolated donor cells from the bone marrow of the recipient mice approximately 10 weeks after transplantation. At this time point, ascorbate-depleted recipient mice showed histological evidence of myeloid leukaemia. Ascorbate depletion reduced 5hmC levels in *Tet2*$^{Δ/+}$;*Flt3*^{ITD} HPC cells and myeloid progenitors (Fig. 4e) without affecting 5mC levels (Fig. 4f). Ascorbate depletion also reduced 5hmC levels in *Tet2*$^{Δ/Δ}$;*Flt3*^{ITD} HPC cells and myeloid progenitors (Fig. 4e, f). This suggests that ascorbate depletion inhibits multiple Tet enzymes in leukaemia cells.

Gulo$^{-/-}$ recipients of *Tet2*$^{Δ/+}$;*Flt3*^{ITD} cells died significantly faster than wild-type recipients (Fig. 4g) and had significantly more myeloblasts, WBCs, blood myeloid cells and spleen HPCs (Fig. 4h–j and Extended Data Fig. 10a, b). Wild-type recipients of *Tet2*$^{Δ/Δ}$;*Flt3*^{ITD} cells had significantly more WBCs (Fig. 4i) than wild-type recipients of *Tet2*$^{Δ/+}$;*Flt3*^{ITD} cells, consistent with the fact that complete loss of Tet2 accelerates leukaemogenesis compared to partial loss of Tet2 (ref. 31). Given that ascorbate depletion reduced Tet2 function (Fig. 2a), these results suggest that ascorbate depletion accelerated leukemogenesis partly by reducing Tet2 function.

Gulo$^{-/-}$ recipients of *Tet2*$^{Δ/Δ}$;*Flt3*^{ITD} cells also died significantly faster than wild-type recipients (Fig. 4g) and had significantly more myeloblasts, WBCs, myeloid cells in their blood, and HPC cells in their spleen (Fig. 4h–j and Extended Data Fig. 10a). Therefore, ascorbate depletion accelerates leukemogenesis partly through Tet2-independent mechanisms that may include regulation of Tet1 or Tet3 (Fig. 4e). We did not detect significant changes in histone methylation markers in leukaemia cells from ascorbate-depleted compared to wild-type mice (Extended Data Fig. 10c). However, ascorbate depletion may promote

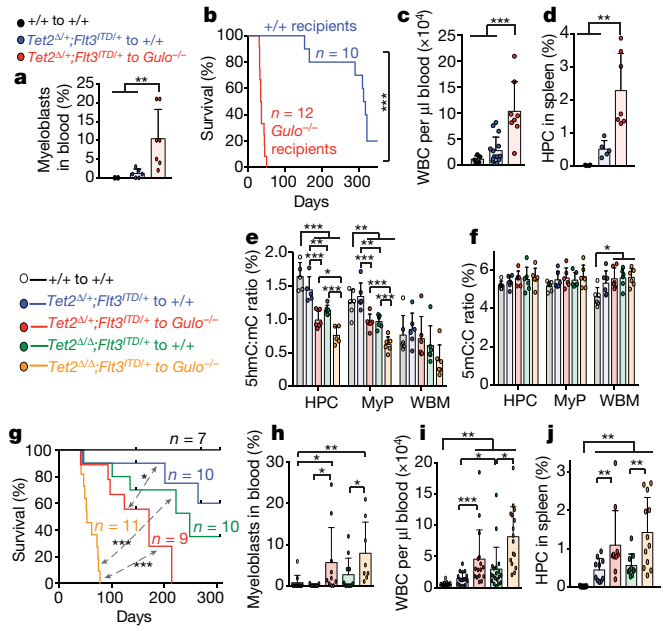

Figure 4 | Low ascorbate levels accelerate leukaemogenesis. a–d, Eight million bone marrow cells from *Tet2*$^{\Delta/+}$;*Flt3*^{ITD} or wild-type donor mice were transplanted into irradiated wild-type or ascorbate-depleted *Gulo*$^{-/-}$ recipient mice and analysed 4–6 weeks after transplantation (a total of three donors with 14–15 recipients per treatment from three independent experiments). **a**, Frequency of myeloblasts in the blood (a total of $n = 2$–7 recipients per treatment). **b**, Kaplan–Meier survival curve of transplant recipients of *Tet2*$^{\Delta/+}$;*Flt3*^{ITD} cells (three independent experiments, Mantel–Cox log-rank test). **c**, **d**, Analysis of the blood or spleen of transplant recipients (a total of $n = 4$–15 recipients per treatment). **e–j**, Eight million bone marrow cells from donor mice of the indicated genotypes were transplanted into irradiated wild-type or ascorbate-depleted *Gulo*$^{-/-}$ recipient mice and analysed 6–8 weeks after transplantation (a total of four donors and 8–19 recipients per treatment from four independent experiments). **e**, **f**, 5hmC:5mC and 5mC:C ratios in donor cells from bone marrow of transplant recipients (a total of $n = 6$ mice per treatment from six independent experiments). **g**, Kaplan–Meier survival curve of transplant recipients (four independent experiments, Mantel–Cox log-rank test). **h-j**, Analysis of the blood or spleen of transplant recipients. Statistical significance was assessed with one-way ANOVAs followed by Fisher's LSD tests (**c–f**, **i**, **j**) or Kruskal–Wallis tests (**a**, **h**). All data represent mean ± s.d. We corrected for multiple comparisons by controlling the false discovery rate. *$P < 0.05$, **$P < 0.01$, ***$P < 0.001$.

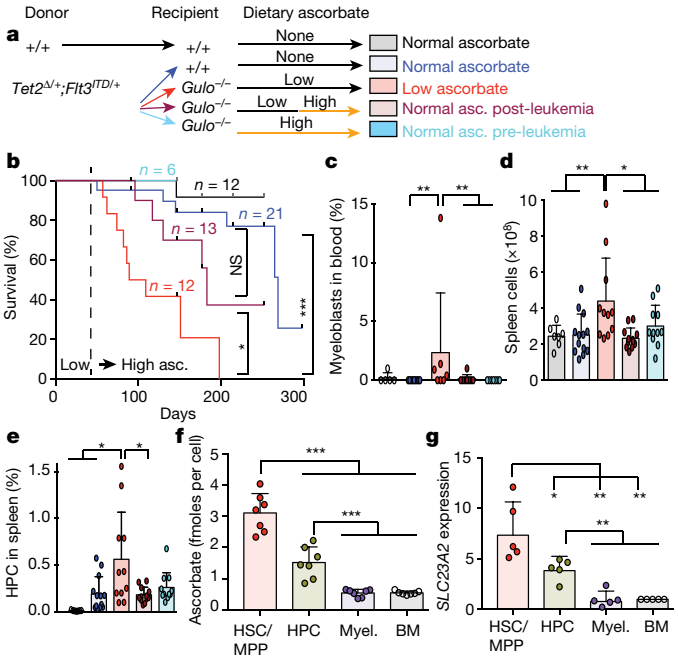

Figure 5 | The effect of ascorbate depletion on leukaemogenesis is reversible and ascorbate levels are high in human HSCs. a–e, Eight million bone marrow cells from *Tet2*$^{\Delta/+}$;*Flt3*^{ITD} or wild-type donor mice were transplanted into irradiated wild-type or *Gulo*$^{-/-}$ recipient mice. Some *Gulo*$^{-/-}$ recipients were fed with ascorbate before (pre-leukaemia) or 6–7 weeks after transplantation (post-leukaemia) (a total of $n = 3$ donors with 5–13 recipients per treatment from four independent experiments). Mice were analysed 10–11 weeks after transplantation. **b**, Kaplan–Meier survival curve of transplant recipients of *Tet2*$^{\Delta/+}$;*Flt3*^{ITD} cells treated (six independent experiments, Mantel–Cox log-rank test). **f**, **g**, Ascorbate levels and *SLC23A2* expression in human bone marrow haematopoietic cells (see Methods for the markers used to isolate each cell population. **f**, A total of $n = 7$ samples analysed from seven independent experiments. **g**, A total of $n = 5$ samples analysed from five independent experiments). Statistical significance was assessed with *t*-tests (**g**), one-way ANOVAs followed by Fisher's LSD tests (**d**, **f**) or Kruskal–Wallis tests (**c**, **e**). We corrected for multiple comparisons by controlling the false discovery rate. All data represent mean ± s.d. *$P < 0.05$, **$P < 0.01$, ***$P < 0.001$.

leukaemogenesis in part by regulating histone demethylases or other dioxygenase enzymes, or through non-cell-autonomous effects on the microenvironment. The relative contribution of Tet2-dependent and Tet2-independent mechanisms to leukemogenesis remains unclear.

We next investigated whether leukaemia progression in an ascorbate-depleted environment can be reversed by dietary ascorbate. Normal ascorbate levels in *Gulo*$^{-/-}$ mice were restored by ascorbate supplementation, starting 6–7 weeks after transplantation (Fig. 5a), when leukaemia was already histologically evident (Fig. 4). Feeding with ascorbate significantly extended survival (Fig. 5b), while significantly reducing myeloblasts in the blood, spleen cellularity and HPC frequency in the spleen (Fig. 5c–e and Extended Data Fig. 10d–f).

To test whether our findings are relevant to humans, we measured ascorbate levels in human haematopoietic cells from fresh adult bone marrow biopsies. Similar to mouse HSCs, human HSCs/MPPs had significantly higher levels of ascorbate (Fig. 5f) and *SLC23A2* expression (Fig. 5g) compared to other haematopoietic cells, and *SLC23A1* expression was not detected. Ascorbate levels in human HSCs (Fig. 5f) were similar to those in mouse HSCs (Fig. 2c).

Addition of ascorbate to the culture medium promotes pluripotency by stimulating Jumonji histone demethylase activity[16] and by stimulating Tet activity[7,22]. Our results do not address the biochemical mechanism by which ascorbate regulates Tet function, but extend the data from cultured cells by showing that physiological variations in ascorbate levels within tissues regulate stem-cell function and cancer initiation.

In western countries, plasma ascorbate levels vary tenfold among individuals[33], and the lowest quartile of men have a significantly higher risk of mortality from cancer[38,39]. Humans with haematological malignancies have substantially lower serum ascorbate levels as compared to healthy controls[40,41]. In clinical trials, oral ascorbate administration failed to benefit patients with established cancers[42], although supra-physiological ascorbate concentrations can slow the growth of some cancers in mice by causing oxidative stress[43,44]. Moreover, clonal haematopoiesis of indeterminate potential is common among older humans and is often associated with loss of one *Tet2* allele[45–47]. Our data suggest that it is important for people with clonal haematopoiesis to get adequate dietary ascorbate to maximize the residual tumour-suppressor function of Tet enzymes.

Online Content Methods, along with any additional Extended Data display items and Source Data, are available in the online version of the paper; references unique to these sections appear only in the online paper.

Received 28 September 2016; accepted 14 August 2017.
Published online 21 August 2017.

1. Garaycoechea, J. I. *et al.* Genotoxic consequences of endogenous aldehydes on mouse haematopoietic stem cell function. *Nature* **489,** 571–575 (2012).
2. Yan, H. *et al. IDH1* and *IDH2* mutations in gliomas. *N. Engl. J. Med.* **360,** 765–773 (2009).
3. Mihaylova, M. M., Sabatini, D. M. & Yilmaz, O. H. Dietary and metabolic control of stem cell function in physiology and cancer. *Cell Stem Cell* **14,** 292–305 (2014).
4. Zhang, H. *et al.* NAD^+ repletion improves mitochondrial and stem cell function and enhances life span in mice. *Science* **352,** 1436–1443 (2016).
5. Agathocleous, M. *et al.* Metabolic differentiation in the embryonic retina. *Nat. Cell Biol.* **14,** 859–864 (2012).
6. Wang, J. *et al.* Dependence of mouse embryonic stem cells on threonine catabolism. *Science* **325,** 435–439 (2009).
7. Blaschke, K. *et al.* Vitamin C induces Tet-dependent DNA demethylation and a blastocyst-like state in ES cells. *Nature* **500,** 222–226 (2013).
8. Carey, B. W., Finley, L. W., Cross, J. R., Allis, C. D. & Thompson, C. B. Intracellular α-ketoglutarate maintains the pluripotency of embryonic stem cells. *Nature* **518,** 413–416 (2015).
9. Naka, K. *et al.* Dipeptide species regulate p38MAPK–Smad3 signalling to maintain chronic myelogenous leukaemia stem cells. *Nat. Commun.* **6,** 8039 (2015).
10. Takubo, K. *et al.* Regulation of glycolysis by Pdk functions as a metabolic checkpoint for cell cycle quiescence in hematopoietic stem cells. *Cell Stem Cell* **12,** 49–61 (2013).
11. Simsek, T. *et al.* The distinct metabolic profile of hematopoietic stem cells reflects their location in a hypoxic niche. *Cell Stem Cell* **7,** 380–390 (2010).
12. May, J. M. The SLC23 family of ascorbate transporters: ensuring that you get and keep your daily dose of vitamin C. *Br. J. Pharmacol.* **164,** 1793–1801 (2011).
13. Seita, J. *et al.* Gene Expression Commons: an open platform for absolute gene expression profiling. *PLoS ONE* **7,** e40321 (2012).
14. Manning, J. *et al.* Vitamin C promotes maturation of T-cells. *Antioxid. Redox Signal.* **19,** 2054–2067 (2013).
15. Young, J. I., Züchner, S. & Wang, G. Regulation of the epigenome by vitamin C. *Annu. Rev. Nutr.* **35,** 545–564 (2015).
16. Wang, T. *et al.* The histone demethylases Jhdm1a/1b enhance somatic cell reprogramming in a vitamin-C-dependent manner. *Cell Stem Cell* **9,** 575–587 (2011).
17. Kivirikko, K. I., Myllylä, R. & Pihlajaniemi, T. Protein hydroxylation: prolyl 4-hydroxylase, an enzyme with four cosubstrates and a multifunctional subunit. *FASEB J.* **3,** 1609–1617 (1989).
18. Rebouche, C. J. Ascorbic acid and carnitine biosynthesis. *Am. J. Clin. Nutr.* **54,** 1147S–1152S (1991).
19. Knowles, H. J., Raval, R. R., Harris, A. L. & Ratcliffe, P. J. Effect of ascorbate on the activity of hypoxia-inducible factor in cancer cells. *Cancer Res.* **63,** 1764–1768 (2003).
20. Vukovic, M. *et al.* Adult hematopoietic stem cells lacking Hif-1α self-renew normally. *Blood* **127,** 2841–2846 (2016).
21. Yin, R. *et al.* Ascorbic acid enhances Tet-mediated 5-methylcytosine oxidation and promotes DNA demethylation in mammals. *J. Am. Chem. Soc.* **135,** 10396–10403 (2013).
22. Chen, J. *et al.* Vitamin C modulates TET1 function during somatic cell reprogramming. *Nat. Genet.* **45,** 1504–1509 (2013).
23. Minor, E. A., Court, B. L., Young, J. I. & Wang, G. Ascorbate induces ten-eleven translocation (Tet) methylcytosine dioxygenase-mediated generation of 5-hydroxymethylcytosine. *J. Biol. Chem.* **288,** 13669–13674 (2013).
24. Ito, S. *et al.* Tet proteins can convert 5-methylcytosine to 5-formylcytosine and 5-carboxylcytosine. *Science* **333,** 1300–1303 (2011).
25. Tahiliani, M. *et al.* Conversion of 5-methylcytosine to 5-hydroxymethylcytosine in mammalian DNA by MLL partner TET1. *Science* **324,** 930–935 (2009).
26. Jan, M. *et al.* Clonal evolution of preleukemic hematopoietic stem cells precedes human acute myeloid leukemia. *Sci. Transl. Med.* **4,** 149ra118 (2012).
27. Moran-Crusio, K. *et al.* Tet2 loss leads to increased hematopoietic stem cell self-renewal and myeloid transformation. *Cancer Cell* **20,** 11–24 (2011).
28. Ko, M. *et al.* Ten-eleven-translocation 2 (TET2) negatively regulates homeostasis and differentiation of hematopoietic stem cells in mice. *Proc. Natl Acad. Sci. USA* **108,** 14566–14571 (2011).
29. Quivoron, C. *et al.* TET2 inactivation results in pleiotropic hematopoietic abnormalities in mouse and is a recurrent event during human lymphomagenesis. *Cancer Cell* **20,** 25–38 (2011).
30. Abdel-Wahab, O. *et al.* Genetic characterization of TET1, TET2, and TET3 alterations in myeloid malignancies. *Blood* **114,** 144–147 (2009).
31. Shih, A. H. *et al.* Mutational cooperativity linked to combinatorial epigenetic gain of function in acute myeloid leukemia. *Cancer Cell* **27,** 502–515 (2015).
32. Delhommeau, F. *et al.* Mutation in *TET2* in myeloid cancers. *N. Engl. J. Med.* **360,** 2289–2301 (2009).
33. Schleicher, R. L., Carroll, M. D., Ford, E. S. & Lacher, D. A. Serum vitamin C and the prevalence of vitamin C deficiency in the United States: 2003–2004 National Health and Nutrition Examination Survey (NHANES). *Am. J. Clin. Nutr.* **90,** 1252–1263 (2009).
34. Pronier, E. *et al.* Inhibition of TET2-mediated conversion of 5-methylcytosine to 5-hydroxymethylcytosine disturbs erythroid and granulomonocytic differentiation of human hematopoietic progenitors. *Blood* **118,** 2551–2555 (2011).
35. Patel, J. P. *et al.* Prognostic relevance of integrated genetic profiling in acute myeloid leukemia. *N. Engl. J. Med.* **366,** 1079–1089 (2012).
36. Cimmino, L. *et al.* TET1 is a tumor suppressor of hematopoietic malignancy. *Nat. Immunol.* **16,** 653–662 (2015).
37. An, J. *et al.* Acute loss of *TET* function results in aggressive myeloid cancer in mice. *Nat. Commun.* **6,** 10071 (2015).
38. Loria, C. M., Klag, M. J., Caulfield, L. E. & Whelton, P. K. Vitamin C status and mortality in US adults. *Am. J. Clin. Nutr.* **72,** 139–145 (2000).
39. Khaw, K. T. *et al.* Relation between plasma ascorbic acid and mortality in men and women in EPIC-Norfolk prospective study: a prospective population study. *Lancet* **357,** 657–663 (2001).
40. Liu, M. *et al.* Vitamin C increases viral mimicry induced by 5-aza-2′-deoxycytidine. *Proc. Natl Acad. Sci. USA* **113,** 10238–10244 (2016).
41. Huijskens, M. J., Wodzig, W. K., Walczak, M., Germeraad, W. T. & Bos, G. M. Ascorbic acid serum levels are reduced in patients with hematological malignancies. *Results Immunol.* **6,** 8–10 (2016).
42. Moertel, C. G. *et al.* High-dose vitamin C versus placebo in the treatment of patients with advanced cancer who have had no prior chemotherapy—a randomized double-blind comparison. *N. Engl. J. Med.* **312,** 137–141 (1985).
43. Yun, J. *et al.* Vitamin C selectively kills *KRAS* and *BRAF* mutant colorectal cancer cells by targeting GAPDH. *Science* **350,** 1391–1396 (2015).
44. Chen, Q. *et al.* Pharmacologic doses of ascorbate act as a prooxidant and decrease growth of aggressive tumor xenografts in mice. *Proc. Natl Acad. Sci. USA* **105,** 11105–11109 (2008).
45. Busque, L. *et al.* Recurrent somatic *TET2* mutations in normal elderly individuals with clonal hematopoiesis. *Nat. Genet.* **44,** 1179–1181 (2012).
46. Genovese, G. *et al.* Clonal hematopoiesis and blood-cancer risk inferred from blood DNA sequence. *N. Engl. J. Med.* **371,** 2477–2487 (2014).
47. Jaiswal, S. *et al.* Age-related clonal hematopoiesis associated with adverse outcomes. *N. Engl. J. Med.* **371,** 2488–2498 (2014).

Supplementary Information is available in the online version of the paper.

Acknowledgements S.J.M. is a Howard Hughes Medical Institute (HHMI) Investigator, the Mary McDermott Cook Chair in Pediatric Genetics, the Kathryn and Gene Bishop Distinguished Chair in Pediatric Research, the director of the Hamon Laboratory for Stem Cells and Cancer, and a Cancer Prevention and Research Institute of Texas Scholar. M.A. was a Royal Commission for the Exhibition of 1851 Research Fellow. We thank F. Harrison for sharing the *Slc23a2*$^{-/-}$ mice, N. Loof and the Moody Foundation Flow Cytometry Facility for flow cytometry, K. Correll, A. Leach and A. Gross for mouse colony management and BioHPC at UT Southwestern for providing high-performance computing. This work was supported by the Cancer Prevention and Research Institute of Texas and the National Institutes of Health (R37 AG024945 and R01 DK100848).

Author Contributions M.A. conceived and performed most experiments. C.E.M. performed experiments with *Tet2*^{fl} and *Tet2*^{fl}*;Flt3*^{ITD} mice in Extended Data Figs 5, 8. R.J.B. and E.P. performed the histone methylation analysis. E.P. and Z.Z. performed RNA-sequencing analysis. Z.Z. performed the statistical analyses. G.M.C. assessed haematopathology in Figs 4, 5. E.B. and B.L.C. provided technical assistance. M.M.M. performed collagen staining. W.C. provided human bone marrow specimens. G.J.S. provided some of the data from *Slc23a2*$^{-/-}$ mice. Z.H., M.A., and R.J.D. developed the metabolomics methods and R.J.D. helped to interpret metabolomics results. M.A. and S.J.M. designed experiments, interpreted results and wrote the manuscript.

Author Information Reprints and permissions information is available at www.nature.com/reprints. The authors declare no competing financial interests. Readers are welcome to comment on the online version of the paper. Publisher's note: Springer Nature remains neutral with regard to jurisdictional claims in published maps and institutional affiliations. Correspondence and requests for materials should be addressed to S.J.M. (Sean.Morrison@UTSouthwestern.edu).

Reviewer Information *Nature* thanks H. Christofk, R. Levine and the other anonymous reviewer(s) for their contribution to the peer review of this work.

METHODS

Mice. *Gulo*$^{-/-}$ (ref. 48), *Tet2*$^{fl/fl}$ (ref. 27), *Flt3*^{ITD} (ref. 49), *Slc23a2*$^{-/-}$ (ref. 50) and *Mx1-cre* (ref. 51) mice were previously described. All mice were on a C57BL/6 background. Both male and female mice were used in all studies. *Tet2*$^{fl/fl}$;*Mx1-cre* mice were injected with five intraperitoneal injections of 20 μg poly(I:C) (GE Healthcare) every other day at 6–8 weeks of age to induce Cre expression. Ascorbate-depleted *Gulo*$^{-/-}$ mice analysed at 6–8 weeks of age were weaned at four weeks of age and then fed a standard mouse diet, which contains little ascorbate. Ascorbate-depleted *Gulo*$^{-/-}$ mice maintained for longer than eight weeks were fed a 1% ascorbate diet (Harlan) from the time of weaning until 6–8 weeks of age, then switched to a standard mouse diet and provided with 100 mg l^{-1} of ascorbate in the drinking water, changed twice per week. This regimen resulted in ascorbate-depleted mice that could be maintained for at least eight months. Ascorbate-replete *Gulo*$^{-/-}$ mice were fed an ascorbate-supplemented diet (a 1% ascorbate diet (Harlan)) from the time of weaning onwards, or as indicated in the text. For the experiments in Fig. 4a–d, *Gulo*$^{-/-}$ mice were fed an ascorbate-supplemented diet until six weeks of age, then switched to a standard mouse diet with 100 mg l^{-1} of ascorbate in the drinking water and transplanted at eight weeks of age. For the experiments in Figs 4e–j, 5a–e, *Gulo*$^{-/-}$ mice were fed an ascorbate-supplemented diet until 10 weeks of age, then switched to a standard mouse diet with 100 mg l^{-1} of ascorbate in the drinking water and transplanted at 12 weeks of age. C57BL/Ka-Thy-1.1 (CD45.2) and C57BL/Ka-Thy-1.2 (CD45.1) mice were used for transplantation experiments. *Gulo*$^{-/-}$;CD45.1 recipient mice were generated by crossing *Gulo*$^{-/-}$ mice with CD45.1 mice. Mice were housed in the Animal Resource Center at the University of Texas Southwestern Medical Center and all procedures were approved by the UT Southwestern Institutional Animal Care and Use Committee.

Cell isolation for experiments other than metabolomics. Cell populations shown in the figures were isolated with the following markers: CD150^{+}CD48^{-}Lineage^{-}Sca-1^{+}Kit^{+} HSCs, CD150^{-}CD48^{-}Lineage^{-}Sca-1^{+}Kit^{+} MPPs, CD48^{+}Lineage^{-}Sca-1^{+}Kit^{+} haematopoietic progenitor cells (HPCs), CD34^{+}CD16/32^{-}Lineage^{-}Sca-1^{-}Kit^{+} common myeloid progenitors (CMPs), CD34^{+}CD16/32^{+}Lineage^{-}Sca-1^{-}Kit^{+} granulocyte–macrophage progenitors (GMPs), CD34^{-}CD16/32^{-}Lineage^{-}Sca-1^{-}Kit^{+} megakaryocyte–erythroid progenitors (MEPs), Mac-1^{+}Gr-1^{+} myeloid cells, CD71^{+}Ter119^{+} erythroid progenitors, and B220^{+}IgM^{+} B cells.

Bone marrow cells were obtained by flushing femurs and tibias with a 25G needle or by crushing femurs, tibias, vertebrae and pelvic bones with a mortar and pestle, in Ca^{2+}- and Mg^{2+}-free Hank's buffered salt solution (HBSS; Gibco), supplemented with 2% heat-inactivated bovine serum (HIBS, Gibco). Spleens and thymuses were dissociated by crushing followed by trituration. All cell suspensions were filtered through a 40-μm cell strainer. Number of cells was measured with a Vi-CELL cell viability analyser (Beckman Coulter) or a haemocytometer. For flow cytometric analysis and isolation, cells were incubated with combinations of antibodies against the following cell-surface markers, conjugated to Pacific Blue, Brilliant Violet 421, Brilliant Violet 510, FITC, PE, PerCP-Cy5.5, PE-Cy5, PE-Cy7, APC, eFluor 660, Alexa Fluor 700, APC-eFluor 780, or biotin: CD2 (RM2-5), CD3ε (17A2), CD4 (GK1.5), CD5 (53-7.3), CD8α (53-6.7), CD11b (M1/70), CD16/32 (93), CD24 (M1/69), CD25 (PC61.5), CD34 (RAM34), CD43 (eBioR2/60), CD44 (IM7), CD45.1 (A20), CD45.2 (104), CD45R (B220; RA3-6B2), CD48 (HM48-1), CD71 (C2), CD117 (Kit; 2B8), CD127 (IL-7Rα; A7R34), CD135 (Flt3; A2F10), CD150 (TC15-12F12.2), Ter119 (TER-119), Sca-1 (D7, E13-161.7), Gr-1 (RB6-8C5), IgM (II/41), F4/80 (BM8). A list of antibodies can be found in Supplementary Table 1. Lineage markers for HSCs and progenitors were CD3, CD5, CD8, B220, Gr-1 and Ter119. Antibody staining was performed at 4 °C for 30 min, or, when CD34 was included in the cocktail, on ice for 90 min. Biotinylated antibodies were visualized by incubation with PE-Cy7-, BV510- or BV421-conjugated streptavidin at 4 °C for 30 min. 4′,6-diamidino-2-phenylindole (DAPI; 2 μg ml^{-1} in phosphate buffered saline (PBS)) or propidium iodide (1 μg ml^{-1}) were used to exclude dead cells during flow cytometry. All reagents were acquired from BD Biosciences, eBiosciences, BioLegend or Tonbo. For isolation of all Kit^{+} cell populations, cells were pre-enriched before flow cytometry using paramagnetic microbeads and an autoMACS magnetic separator (Miltenyi Biotec). Analysis and cell sorting were performed using a FACSAria flow cytometer (BD Biosciences) or a BD FACSCanto (BD Biosciences). Data were analysed using FACSDiva (BD Biosciences).

Cell isolation for metabolomics. Methods for the isolation of cells for metabolomics were optimized for speed and to keep the cells cold at all times, to minimize metabolic changes during isolation. Mice were euthanized by cervical dislocation and bone marrow cells were obtained by crushing femurs, tibias, vertebrae and pelvic bones with an ice-cold mortar and pestle in a 4 °C cold room or on ice in 2 ml of Ca^{2+}- and Mg^{2+}-free HBSS, supplemented with 0.5% bovine serum albumin. Cells were filtered through a 40-μm cell strainer or a 45-μm nylon mesh into 5-ml tubes on ice. For sorting haematopoietic stem and progenitor cells, paramagnetic MicroBeads against Kit (Miltenyi) were added to each sample, followed 1 min later by all of the antibodies used for the isolation of the relevant cell populations (as indicated). Fluorochrome-conjugated antibodies were used in all cases to enable a single staining step. For experiments in which CD45^{+} bone marrow cells were isolated, paramagnetic MicroBeads against CD45 (Miltenyi) were used to pre-enrich, followed 1 min later by the other antibodies required to isolate the other cell populations in the experiment. Antibody staining was for 30 min on ice in a 4 °C cold room, with occasional mixing. Then Kit^{+} cells or CD45^{+} cells were enriched using a QuadroMACS manual separator (Miltenyi) in the cold room. For most experiments, four mice were analysed in parallel, in which case the total time from killing the first mouse to the completion of cell isolation was 2–3 h, during which time the samples were kept on ice as each sample was processed. Control experiments showed that incubation for up to 7 h on ice did not significantly change the levels of most of the metabolites that we detected in bone marrow cells (Extended Data Fig. 1b). Cells were sorted on a FACSAria flow cytometer running with a sheath fluid of 0.5× PBS, prepared fresh using Milli-Q water (Millipore), and a 70-μm nozzle in a four-way purity sort mode to minimize the volume of sorted drops, so as to eliminate ion suppression of mass spectrometry signals from salts in the sheath fluid. The FACSAria sheath tank was washed with Milli-Q deionized water before the experiment to eliminate contaminants and dedicated glassware was used to make all buffers. Each sample was in HBSS + 0.5% BSA and kept at 4 °C during sorting, which lasted about 20 min per sample. Equal numbers of cells from each population were directly sorted in each experiment (usually 5,000–20,000 cells) into 500 μl of cold 80% methanol pre-chilled on dry ice and maintained at 4 °C during sorting. No serum was used during the procedure. After sorting, each sample was kept on dry ice for the duration of the experiment, and then stored at −80 °C.

Metabolite extraction and metabolomics. Samples in 80% methanol were vortexed for 1 min to lyse the cells, then centrifuged at 17,000*g* for 15 min at 4 °C. To measure ascorbate, 15 pmoles ^{13}C-ascorbate (Sigma-Aldrich) was added to the 80% methanol as an internal standard and 1 mM EDTA was added to prevent ascorbate oxidation[52]. Cell extracts were centrifuged immediately after cell isolation. The supernatant was transferred to a new tube and lyophilized using a Speedvac (Thermo Scientific). Dried metabolites were reconstituted in 30 μl of 0.03% formic acid, vortexed, centrifuged at 17,000*g* for 15 min at 4 °C and the supernatant was analysed using liquid chromatography–tandem mass spectrometry (LC–MS/MS). For experiments in which ascorbate was measured in cells, dried metabolites were reconstituted in 30 μl of 0.03% formic acid + 1 mM EDTA. For experiments in which ascorbate was measured in the plasma, four volumes of 90% methanol + 1 mM EDTA + ^{13}C-ascorbate on dry ice were added to one volume of plasma, vortexed, centrifuged at 17,000*g* for 15 min at 4 °C and the supernatant analysed by LC–MS/MS. A Nexera Ultra High Performance Liquid Chromatograph (UHPLC) system (Shimadzu) was used for liquid chromatography, with a Polar-RP HPLC column (150 × 2 mm, 4 μm, 80 Å, Phenomenex) and the following gradient: 0–3 min 100% mobile phase A; 3–15 min 100–0% A; 15–17 min 0% A; 17–18 min 0–100% A; 18–23 min 100% A. Mobile Phase A was 0.03% formic acid in water. Mobile Phase B was 0.03% formic acid in acetonitrile. The flow rate was 0.5 ml min^{-1}, the column was at 35 °C and the samples in the autosampler were at 4 °C. Mass spectrometry was performed with a triple quadrupole mass spectrometer (AB Sciex QTRAP 5500) in multiple reaction monitoring (MRM) mode as described[53], with some modifications. Transitions that never gave a signal in extracts from 20,000 cells were omitted from the MRM list. For experiments to detect ascorbate, the dwelling time for ascorbate and ^{13}C-ascorbate was increased to 50 ms. Chromatogram peak areas were integrated using Multiquant (AB Sciex). For analysis, the peak area for each metabolite was normalized to the median peak area of the sample. For hierarchical clustering, only metabolites that were detected in every cell population were used. Metabolomics data analysis and hierarchical clustering were performed using MetaboAnalyst[54] and Simca (Umetrics).

Measurement of 5hmC, 5mC and C by LC–MS/MS. To measure modified cytosines in purified populations, cells were sorted by flow cytometry into Ca^{2+} and Mg^{2+} free HBSS + 2% heat inactivated bovine serum, washed once with ice cold normal saline, and the genomic DNA was purified using the QIAamp micro kit (Qiagen) according to the manufacturer's instructions. To measure modified cytosines in unfractionated bone marrow, 5 million fresh bone marrow cells were pelleted, washed once with ice cold normal saline and genomic DNA was purified using the DNeasy blood and tissue kit (Qiagen) according to the manufacturer's instructions. Total genomic DNA from sorted cells, or 1 μg of DNA from unfractionated bone marrow, was digested to nucleosides with DNA Degradase Plus (Zymo Research), according to the manufacturer's instructions, with the following internal standards added to the mix: ^{13}C-^{15}N$_2$-2-deoxycytidine (^{13}C-^{15}N$_2$-2dC), D3-5-methyl-2-deoxycytidine (D3-5mdC), D3-5-hydroxymethyl-2-deoxycytidine (D3-5hmdC) (Toronto Research Chemicals). Samples were then filtered with a

10 kDa Amicon column (Millipore) to remove enzymes, and filtrates were analysed by LC–MS/MS. Liquid chromatography was carried out with a Waters Atlantis or a Scherzo SM-C18 (Imtakt) reverse phase C18 column, 3 μm, 2.1 × 100 mm. Mobile phase A was 0.1% formic acid in water, and mobile phase B was 0.1% formic acid in acetonitrile. The gradient was: 0–2.5 min 0% B; 2.5–5 min 0–100% B; 5–6 min 100% B; 6–7 min 100–0% B; 7–9 min 0% B. The flow rate was 0.5 ml min^{-1}. The flow was diverted to the waste for the first 0.9 min. The column was at 35 °C and the samples in the autosampler were at 4 °C. Mass spectrometry was performed with an AB Sciex QTRAP 5500 operating in MRM mode. Mass spectrometry parameters were optimized using pure standards for 2-deoxycytidine (2dC), 5-methyl-2-deoxycytidine (5mdC) and 5-hydroxymethyl-2-deoxycytidine (5hmdC) (Berry and Associates). The following transitions were monitored in positive mode: 2dC 228.1/112.1; 5mdC 242.1/126.1; 5hmdC 258.1/142.1; ^{13}C-$^{15}N_2$-2dC, 231.1/115.1; D3–5mdC 245.1/129.1; D3–5hmdC 261.1/145.1. Calibration curves of different amounts of pure standards were run to ensure linearity of measurements. Chromatogram peak areas were integrated using Multiquant (AB Sciex). The amount of each nucleoside in a sample was calculated by dividing the peak area of the unlabelled endogenous nucleoside by the peak area of the labelled internal standard.

Bone marrow reconstitution assays. Recipient mice (CD45.1) were irradiated using an XRAD 320 X-ray irradiator (Precision X-Ray Inc.) with two doses of 540 rad (1,080 rad in total) delivered at least 3 h apart. Cells were injected into the retro-orbital venous sinus of anaesthetized recipients. For competitive transplants, mixed donor (CD45.2) and competitor (either CD45.1 or CD45.1/CD45.2) cells were transplanted. After transplantation, mice were maintained on antibiotic water (Baytril 0.08 mg ml^{-1}) for 2–4 weeks. Blood was obtained from the tail veins of recipient mice every four weeks for at least 16 weeks after transplantation. Red blood cells were lysed with ammonium chloride potassium buffer. The remaining cells were stained with antibodies against CD45.2, CD45.1, CD45R (B220), CD11b, CD3 and Gr-1 and analysed by flow cytometry. For the non-competitive bone marrow transplants in Figs 4, 5, 8×10^6 CD45.2 or CD45.2/CD45.1 bone marrow cells were transplanted into irradiated CD45.1 recipients. For the secondary bone marrow transplants in Extended Data Fig. 8h, 5 million bone marrow cells from primary recipients were transplanted into irradiated CD45.1 secondary recipients.

BrdU incorporation analysis. Mice were injected with a single dose of 5-bromo-2′-deoxyuridine (BrdU; 1 mg per 10 g body mass) and maintained on 1 mg BrdU per ml drinking water for three days. Then HSCs or MPPs were isolated as described above, fixed, and stained using the BrdU APC Flow Kit (BD Biosciences) and analysed for BrdU incorporation. For the other cell populations analysed, which are more abundant than HSCs and MPPs, cells were stained with cell surface antibodies, then fixed and stained using the BrdU APC Flow Kit (BD Biosciences) and analysed for BrdU incorporation.

Human haematopoietic cell purification. Bone marrow aspirates were collected from patients, aged 34–85, who were being assessed for lymphoma, for whom no evidence of lymphoma or myelodysplastic syndrome was observed. Each sample was obtained from a different patient. Following diagnosis, aspirates were stained using antibodies against CD34 (4H11, APC-conjugated), CD45RA (HI100, PE-conjugated), CD38 (HIT2, PECy7-conjugated), and Lineage markers (CD2, CD3, CD14, CD16, CD19, CD56, CD235A, Thermo Fisher, FITC-conjugated). The cells were purified within 1–2 days of the biopsy. Prior to purification, bone marrow aspirates were kept at 4 °C in RPMI medium. The cell populations shown in Fig. 5 were isolated with the following markers: $Lin^-CD34^+CD38^-CD45RA^-$ cells (a population enriched in HSCs/MPPs[55]), $Lin^-CD34^+CD38^+$ cells (enriched in restricted haematopoietic progenitors[55]), $CD13^+CD33^+$ myeloid cells and unfractionated cells. This study was approved by the Institutional Review Board of the University of Texas Southwestern Medical Center (IRB STU 122013-023).

PCR and quantitative PCR. PCR Genotyping primers: *Gulo*: 5′-CCCAGTGACTAAGGATAAGC-3′, 5′-CGCGCCTTAATTAAGGATCC-3′, 5′-GTCGTGACAGAATGTCTTGC-3′. Wild-type band = 343 bp, knockout band = 230 bp. *Slc23a2*$^-$: 5′-GGCAGTGTTGGTCCTTCTGT-3′, 5′-CTGGCTATCCTCGTGTCCTG-3′, 5′-CTTAAACCATGGGGCTACCA-3′, 5′-AGACTGCCTTGGGAAAAGCG-3′, wild-type band = 140 bp, knockout band = 180 bp. *Tet2*$^{fl/fl}$ and *Flt3*^{ITD} genotyping were as previously described[27,49].

For qPCR, cells were sorted into RLT buffer (Qiagen RNAeasy Micro kit) and RNA was purified according to the manufacturer's instructions. cDNA was made with iScript reverse transcriptase (BioRad) and quantitative PCR was performed with iTaq Universal SYBR Green (BioRad) and a LightCycler 480 (Roche Applied Science). The signal from each sample was normalized to β-actin. qPCR primers: mouse *Slc23a2*: 5′-GGACAACACCATCCCAGGTA-3′, 5′-CCTTTGCTCACACCCTTCTT-3′. Mouse *Slc23a1*: 5′-GAAGCCACCTCAATGAAAGG-3′, 5′-GCTGAGATCTCCAACTCAGGTC-3′. Mouse β-actin (*Actb*): 5′-CACTGTCGAGTCGCGTCC-3′, 5′-TCATCCATGGCGAACTGGTG-3′. Human *SLC23A2*: 5′-CTGCAGCCAGCTAGGTCTTG-3′, 5′-AAGCTAGGAGCCCAGGATCA-3′. Human *SLC23A1*: 5′-TCCTCCTCCTTGGCCTTTGT-3′, 5′-CCCTGGTGGTTTCATGCTGT-3′. Human β-Actin (*ACTB*): 5′-ATTGGCAATGAGCGGTTC-3′, 5′-CGTGGATGCCACAGGACT-3′.

RNA-sequencing (RNA-seq) analysis. Cells were sorted into RLT buffer (Qiagen RNAeasy Plus Micro kit) and RNA was purified according to the manufacturer's instructions. RNA quality was validated using a Pico Bioanalyzer. RNA sequencing libraries were generated using the SMARTer Stranded Total RNA-Seq kit, Pico Input Mammalian (Clonetech). Library fragment size was measured using D1000 Screen Tape (Agilent) and library concentration was measured using the Qubit RNA assay kit (Life Technologies). Libraries were sequenced using the Illumina NextSeq 500 desktop Next Generation Sequencing system. The quality of RNA-seq raw reads was checked using FastQC v.0.11.2. Raw reads were quality-trimmed using Trimmomatic v.0.32 and mapped to the mouse genome, GRCm38, using TopHat v.2.0.12 with Bowtie2 v.2.2.3. Mapped reads were quality-filtered using SAMtools v.0.1.19, and quantified using HTSeq v.0.6.1. Differential expression was assessed using DESeq2 v.1.8.2 and RUVSeq v.1.2.0 with R v.3.2.1. A fold-change heat map was generated using Cluster 3.0. Computational analysis was performed using the BioHPC high-performance computing cluster at UTSW.

HSC culture. 10 HSCs per well were sorted into a 96-well plate containing IMDM with 10% fetal bovine serum, 50 ng ml^{-1} SCF, 10 ng ml^{-1} TPO, 10 ng ml^{-1} IL-3 and 4 ng ml^{-1} IL-6. For experiments that assessed erythroid differentiation (Extended Data Fig. 6m), 2 U ml^{-1} EPO was included. Ascorbate or 2-phospho-ascorbate (Sigma-Aldrich) were used at 50 μg ml^{-1}. The culture medium was changed every two days. Eight days after plating, cells were stained and analysed by flow cytometry.

Histology. Routine histological processing of tissue specimens was performed at the UTSW Molecular Pathology Core. Sirius red and Masson's trichrome stains on paraffin bone sections were performed according to the supplier's instructions (IHCWorld). With Sirius red, collagen is stained red with bright field imaging, and stained red or green with polarized light imaging. With Masson's trichrome, collagen is stained blue. Blood smears were stained with Diff-Quik. Peripheral blood was subjected to an automated complete blood count, and, where indicated, a manual WBC differential was performed by a haematopathologist (G.M.C.) to assess blast percentage. Criteria from ref. 56 were used for assessment of myeloid leukaemias in Figs 4, 5.

Reactive oxygen species (ROS) staining. For ROS staining, 5 million cells were stained with cell surface antibodies as described above. They were then washed and stained with CellRox DeepRed (Life Technologies) or using the ROS-ID ROS/Superoxide detection kit (Enzo) for 30 min at 37 °C in Ca^{2+}- and Mg^{2+}-free HBSS + 2% HIBS + 50 μM verapamil (Sigma-Aldrich), then washed and analysed by flow cytometry.

Protein extraction and western blot analysis. Equal numbers of cells from each population were sorted into trichloroacetic acid (TCA, Sigma-Aldrich), and the TCA final concentration was adjusted to 10%. Samples were centrifuged at 16,000*g* for 15 min, and precipitates were washed twice with cold acetone and dried. Samples were solubilized in 9 M urea, 2% Triton X-100, 1% DTT. LDS loading buffer (Life Technologies) was added. Samples were heated at 70 °C for 10 min, separated on NuPAGE Bis-Tris polyacrylamide gels (Life Technologies), and transferred to 0.2 μm PVDF membranes (BioRad) by wet transfer using NuPAGE transfer buffer (Life Technologies). Western blots were performed using antibodies against β-actin (AC-74, Sigma-Aldrich), histone H3 (polyclonal, Abcam, ab1791), H3K4me3 (C42D8, Cell Signaling), H3K27me3 (C36B11, Cell Signaling), H3K4me2 (C75H12, Cell Signaling) and H3K36me2 (C64G9, Cell Signaling). For low numbers of cells (7,000–15,000), the SuperSignal Western Blot Enhancer kit (Thermo Scientific) was used according to the manufacturer's instructions. Signals were detected using the SuperSignal West Pico or SuperSignal West Femto chemiluminescence kits (Thermo Scientific). Blots were stripped with 0.2 N NaOH and/or 1% SDS, 25 mM glycine, pH = 2 before re-probing.

Statistical methods. Most figure panels contain data from multiple independent experiments performed on different days. Data represent mean ± standard deviation, except when data are presented as fold-change values, in which case the geometric mean ± geometric standard deviation is shown. Numbers of experiments noted in figure legends reflect independent experiments that were almost always performed on different days. The sample size used in each experiment was not predetermined or formally justified for statistical power. For samples with low variation, for example, metabolite levels in HSCs, 4–6 samples per condition were analysed in each experiment. For samples with large variation, for example, transplantation experiments, 15–20 samples per condition were analysed in each experiment. Blinding was not used in experiments. Mice were allocated to experiments randomly and samples processed in an arbitrary order, but formal randomization techniques were not used.

Prior to analysing the statistical significance of differences among treatments we tested whether data were normally distributed and whether variance was similar among treatments. To test for normality, we performed the D'Agostino–Pearson omnibus test for sample sets with $n > 8$ or the Shapiro–Wilk normality test for smaller sample sets. To test whether variability significantly differed among treatments we performed *F*-tests (for experiments with two treatments) or Levene's median tests (for experiments with more than two treatments). When the data significantly deviated from normality ($P < 0.01$) or variability significantly differed among treatments ($P < 0.05$), we $\log_2$-transformed the data and tested again for normality and variability. If the transformed data no longer significantly deviated from normality and equal variability, we then performed parametric tests on the transformed data. If the transformed data still significantly deviated from normality or equal variability, we performed non-parametric tests on the non-transformed data.

To assess the statistical significance of a difference between two treatments, we used two-tailed Student's *t*-tests (when a parametric test was appropriate), Mann–Whitney *U*-tests (when the data in any treatment significantly deviated from normality) or Welch's tests (when the data were normally distributed, but variances were unequal among treatments). To assess the statistical significance of differences between more than two treatments, we used one-way or two-way ANOVAs (when a parametric test was appropriate; two-way ANOVAs were used when the experiment involved multiple genotypes as well as multiple time points or multiple cell populations) or Kruskal–Wallis tests (when the data in any treatment significantly deviated from normality or variances were unequal among treatments).

For ANOVAs in which a minority of samples significantly diverged from normality or equal variance, ANOVAs were used followed by Mann–Whitney *U*-tests or Kruskal–Wallis tests for comparisons that involved the abnormal groups. To test overall differences among genotypes in transplantation experiments, we used either a mixed two-way ANOVA in which data from the same mouse across time points were taken as repeated measurements (when data were normally distributed and equally variable), or a non-parametric mixed model statistical method, nparLD[57] (when some of the data significantly deviated from normality or equal variability). To confirm the results of the nparLD method, we also performed mixed two-way ANOVAs. Differences that were significant by the nparLD method were almost always significant by the mixed two-way ANOVA. We always corrected for multiple comparisons using the false discovery rate method with the two-stage linear step-up procedure of Benjamini, Krieger and Yekutieli.

The statistical significance of differences in survival was assessed using the Mantel–Cox log-rank test. The statistical significance of differences in fold-change values was assessed using $\log_2$-transformed data. For analysis of metabolomics data, the raw value for each metabolite was normalized to the median metabolite value in each sample. Normalization to the average metabolite value of each sample was also performed to ensure relative values between samples were consistent, independent of the mode of normalization. All statistical analyses were performed with Graphpad Prism software with the exception of the nparLD test, which was performed with R v.3.2.1.

The only mice excluded from experiments were transplant recipients that had no donor cell reconstitution in Fig. 3e and Extended Data Fig. 8g. Because only 1 in 37,000 whole bone marrow cells in wild-type mice is an HSC[58], and HSC frequency in $Flt3^{ITD}$ mice was 5–10-fold lower than in wild-type mice (Extended Data Fig. 8a), it was expected that some recipients of 300,000 (Extended Data Fig. 8g) or 500,000 (Fig. 3e) whole bone marrow cells from these genotypes would receive no HSCs. Therefore, for purposes of comparing donor cell reconstitution levels among treatments, we only included recipient mice with at least 1% donor cell reconstitution, and excluded recipients with <1% donor cell reconstitution (6 out of 23 $Flt3^{ITD}$ recipients, 8 out of 19 $Tet2^{\Delta/+};Flt3^{ITD}$ recipients and 3 out of 9 $Tet2^{\Delta/\Delta};Flt3^{ITD}$ recipients were excluded from the experiment shown in Extended Data Fig. 8g; 5 out of 20 $Tet2^{\Delta/\Delta};Flt3^{ITD}$ to wild-type recipients and 5 out of 20 $Tet2^{\Delta/\Delta};Flt3^{ITD}$ to $Gulo^{-/-}$ recipients were excluded from the experiment in Fig. 3e). In Fig. 5f, samples from one patient were excluded, because of evidence of myelodysplastic syndrome. In Extended Data Fig. 6d, data from the four week time point were excluded from the statistical analysis, because mice had not yet been treated with poly(I:C) and therefore the cells were not yet *Tet2* deficient.

Data availability. RNA-seq data have been submitted to the Sequence Read Archive (SRA) with BioProject accession number PRJNA391832 and SRA accession number SRP110757. The Source Data contain the numeric data for all figures and extended data figures.

48. Maeda, N. *et al.* Aortic wall damage in mice unable to synthesize ascorbic acid. *Proc. Natl Acad. Sci. USA* **97,** 841–846 (2000).
49. Lee, B. H. *et al.* FLT3 mutations confer enhanced proliferation and survival properties to multipotent progenitors in a murine model of chronic myelomonocytic leukemia. *Cancer Cell* **12,** 367–380 (2007).
50. Sotiriou, S. *et al.* Ascorbic-acid transporter Slc23a1 is essential for vitamin C transport into the brain and for perinatal survival. *Nat. Med.* **8,** 514–517 (2002).
51. Kühn, R., Schwenk, F., Aguet, M. & Rajewsky, K. Inducible gene targeting in mice. *Science* **269,** 1427–1429 (1995).
52. Washko, P. W., Welch, R. W., Dhariwal, K. R., Wang, Y. & Levine, M. Ascorbic acid and dehydroascorbic acid analyses in biological samples. *Anal. Biochem.* **204,** 1–14 (1992).
53. Mullen, A. R. *et al.* Oxidation of alpha-ketoglutarate is required for reductive carboxylation in cancer cells with mitochondrial defects. *Cell Reports* **7,** 1679–1690 (2014).
54. Xia, J., Sinelnikov, I. V., Han, B. & Wishart, D. S. MetaboAnalyst 3.0—making metabolomics more meaningful. *Nucleic Acids Res.* **43,** W251–W257 (2015).
55. Doulatov, S. *et al.* Revised map of the human progenitor hierarchy shows the origin of macrophages and dendritic cells in early lymphoid development. *Nat. Immunol.* **11,** 585–593 (2010).
56. Kogan, S. C. *et al.* Bethesda proposals for classification of nonlymphoid hematopoietic neoplasms in mice. *Blood* **100,** 238–245 (2002).
57. Noguchi, K., Gel, Y. R., Brunner, E. & Konietschke, F. NparLD: an R software package for the nonparametric analysis of longitudinal data in factorial experiments. *J. Stat. Softw.* **50,** 1–23 (2012).
58. Acar, M. *et al.* Deep imaging of bone marrow shows non-dividing stem cells are mainly perisinusoidal. *Nature* **526,** 126–130 (2015).

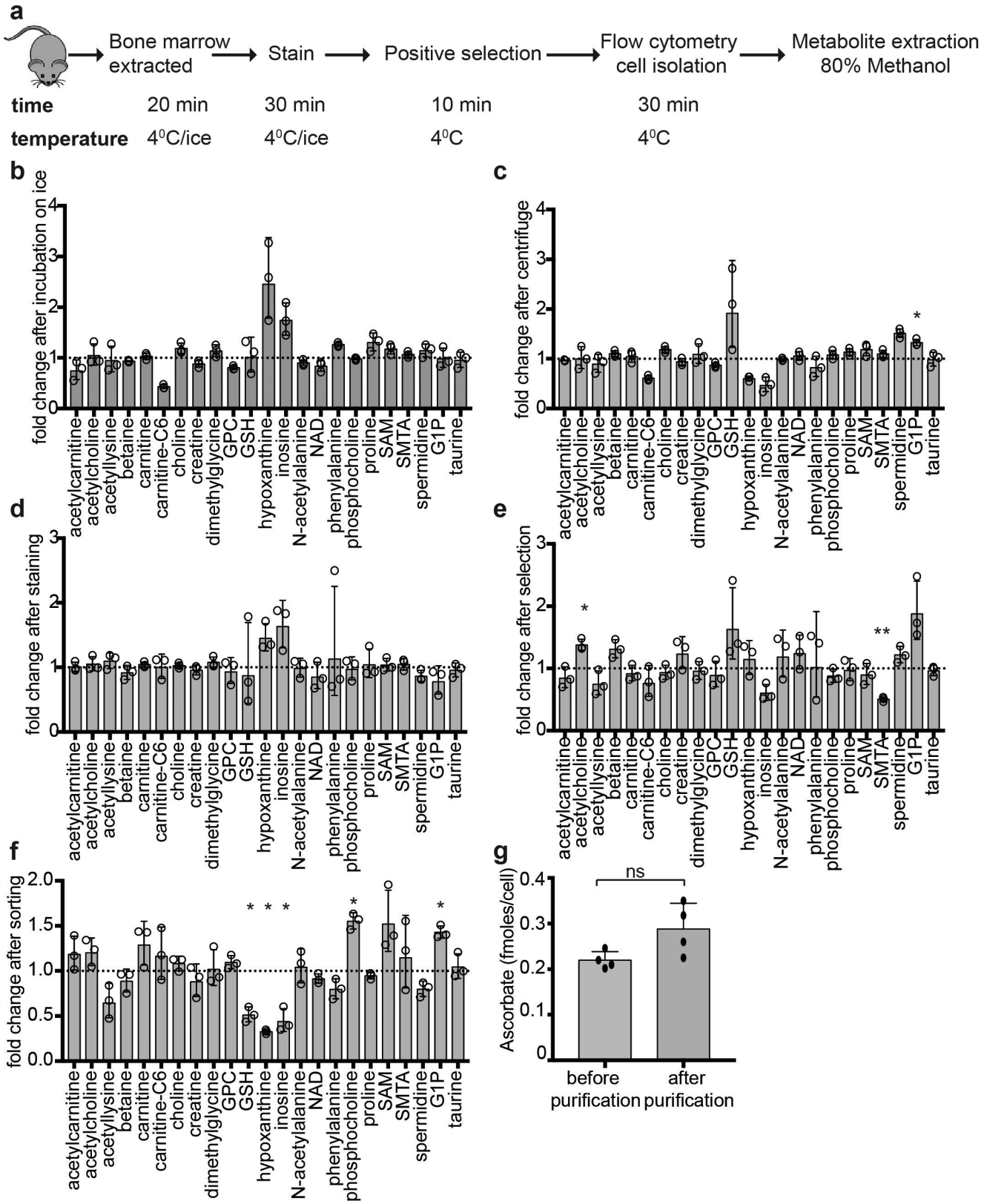

Extended Data Figure 1 | See next page for caption.

Extended Data Figure 1 | Stability of metabolites during cell isolation. **a**, Diagram of the isolation procedure. **b**–**f**, Fold changes in the levels of representative metabolites in 20,000 bone marrow cells before and after each step of the cell isolation procedure. Metabolites were extracted before and after bone marrow cells were kept on ice for 7 h (**b**), centrifuged at 4 °C at 300*g* for 5 min (**c**), stained with the antibodies used for HSC isolation (**d**), cells underwent positive selection with anti-CD45 and anti-Ter119 beads (**e**) or were sorted by flow cytometry for CD45 and Ter119 (**f**). G1P, glucose/fructose-1-phosphate; GPC, glycerophosphocholine; GSH, glutathione; NAD, nicotinamide adenine dinucleotide; SAM, *S*-adenosylmethionine; SMTA, *S*-methyl-5′-thioadenosine. Although most bone marrow cells are $CD45^+$ or $Ter119^+$, unfractionated samples are different in cellular composition from samples after selection and sorting, perhaps contributing to the changes observed in some metabolites in **e** and **f**. Data were normalized to the median metabolite signal intensity of each sample. Statistical significance was assessed with *t*-tests performed on $\log_2$-transformed data. We accounted for multiple comparisons by controlling the false discovery rate. $n = 3$ mice; $^*P < 0.05$, $^{**}P < 0.01$, $^{***}P < 0.001$. **g**, Ascorbate levels were compared in whole bone marrow cells from which metabolites were extracted before the cell purification procedure, or after flow cytometric purification (a total of $n = 4$ mice from two independent experiments). Statistical significance was assessed using a paired *t*-test. All data represent mean ± s.d. ns, not significant.

a

metabolic pathway	# detected
nucleotide	17
amino acid	15
central carbon	5
polyamines	2
redox	3
methylation/choline	8
carnitine	5
vitamins	4
Total	59

b

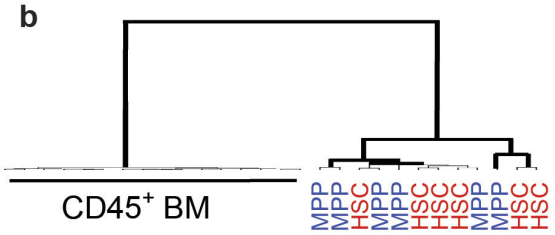

c

Metabolites enriched in HSCs vs CD45⁺ BM

metabolite	fold change	± stdev	q (FDR)
glycerophosphocholine	34	8.7	<0.0001
ascorbate	18	14	0.0001
phosphocholine	2.7	1.9	<0.0001
choline	2.1	0.5	<0.0001
GSH	2.0	1.7	0.002

Metabolites depleted in HSCs vs BM

metabolite	fold change	± stdev	p (FDR)
glutamine	0.18	0.13	<0.0001
N-acetylaspartate	0.30	0.23	<0.0001
hypoxanthine	0.34	0.17	<0.0001
carnitine	0.36	0.31	<0.0001
IMP	0.36	0.04	0.0003
spermidine	0.38	0.17	<0.0001
acetylcholine	0.42	0.26	0.002
trimethyllysine	0.48	0.25	<0.0001
betaine	0.50	0.16	<0.0001
glutamate	0.64	0.10	<0.0001
taurine	0.77	0.11	0.0001

d

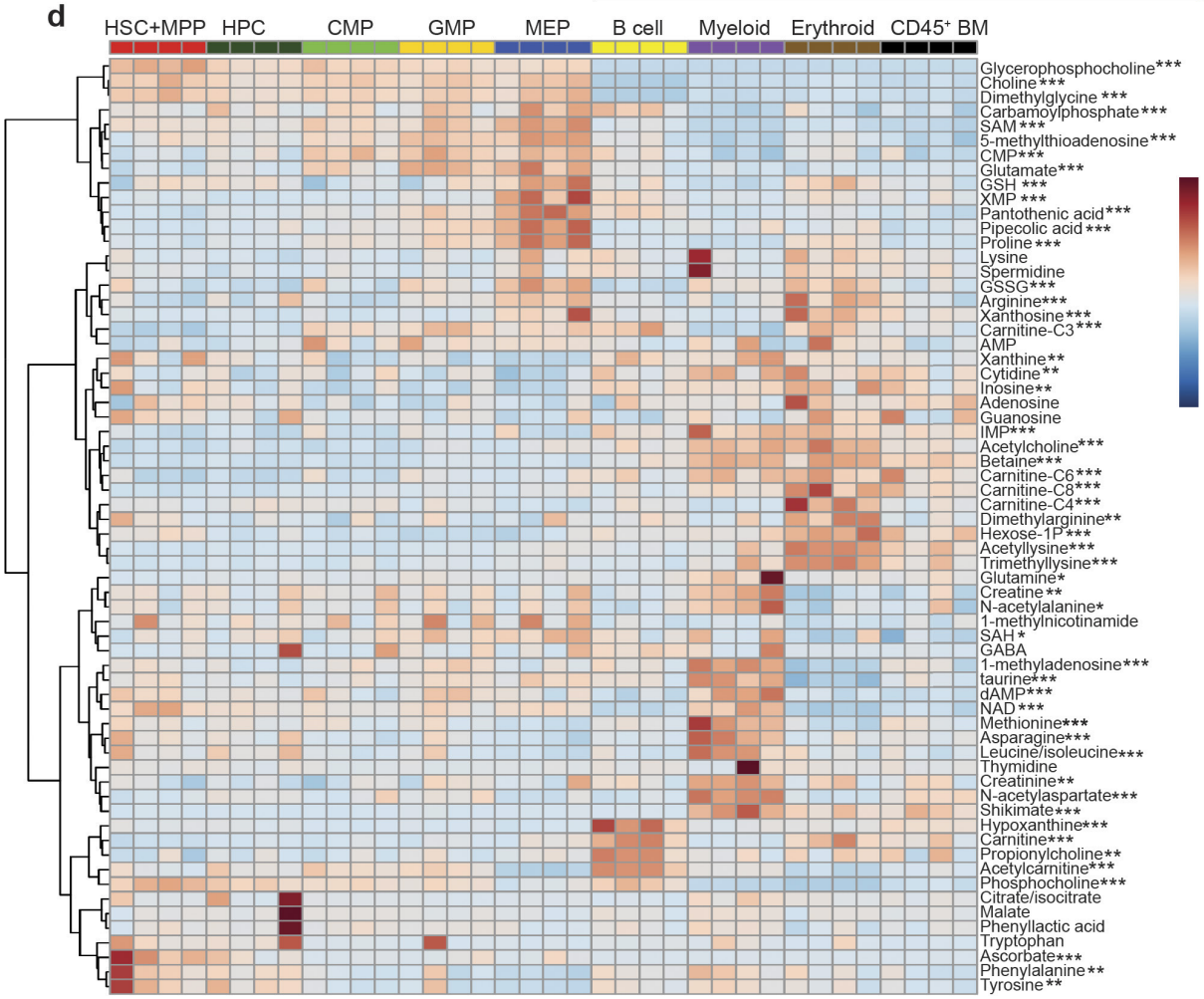

Extended Data Figure 2 | Differences in metabolite levels among haematopoietic stem and progenitor cell populations in the bone marrow. a, Types of metabolites detected in 10,000 HSCs. **b**, Unsupervised clustering of metabolomic data from HSCs, MPPs and CD45$^+$ bone marrow haematopoietic cells isolated from six independent experiments. BM, bone marrow. **c**, Metabolites that significantly differed between HSCs and CD45$^+$ bone marrow cells (six independent experiments with a total of 6 HSC samples and 16 CD45$^+$ bone marrow samples). GSH, glutathione; IMP, inosine monophosphate. Statistical significance was assessed using *t*-tests performed on $\log_2$-transformed data. We accounted for multiple comparisons by controlling the false discovery rate. All data represent mean ± s.d. **d**, The metabolites that we measured in stem and progenitor cell populations. The display is autoscaled for each metabolite to illustrate changes across samples. In total, 52 out of 64 metabolites show statistically significant changes among at least some cell populations (one experiment is shown, representative of three independent experiments; $^*P < 0.05$, $^{**}P < 0.01$, $^{***}P < 0.001$) assessed using a one-way ANOVA for each metabolite followed by Fisher's LSD tests corrected for multiple comparisons by controlling the false discovery rate.

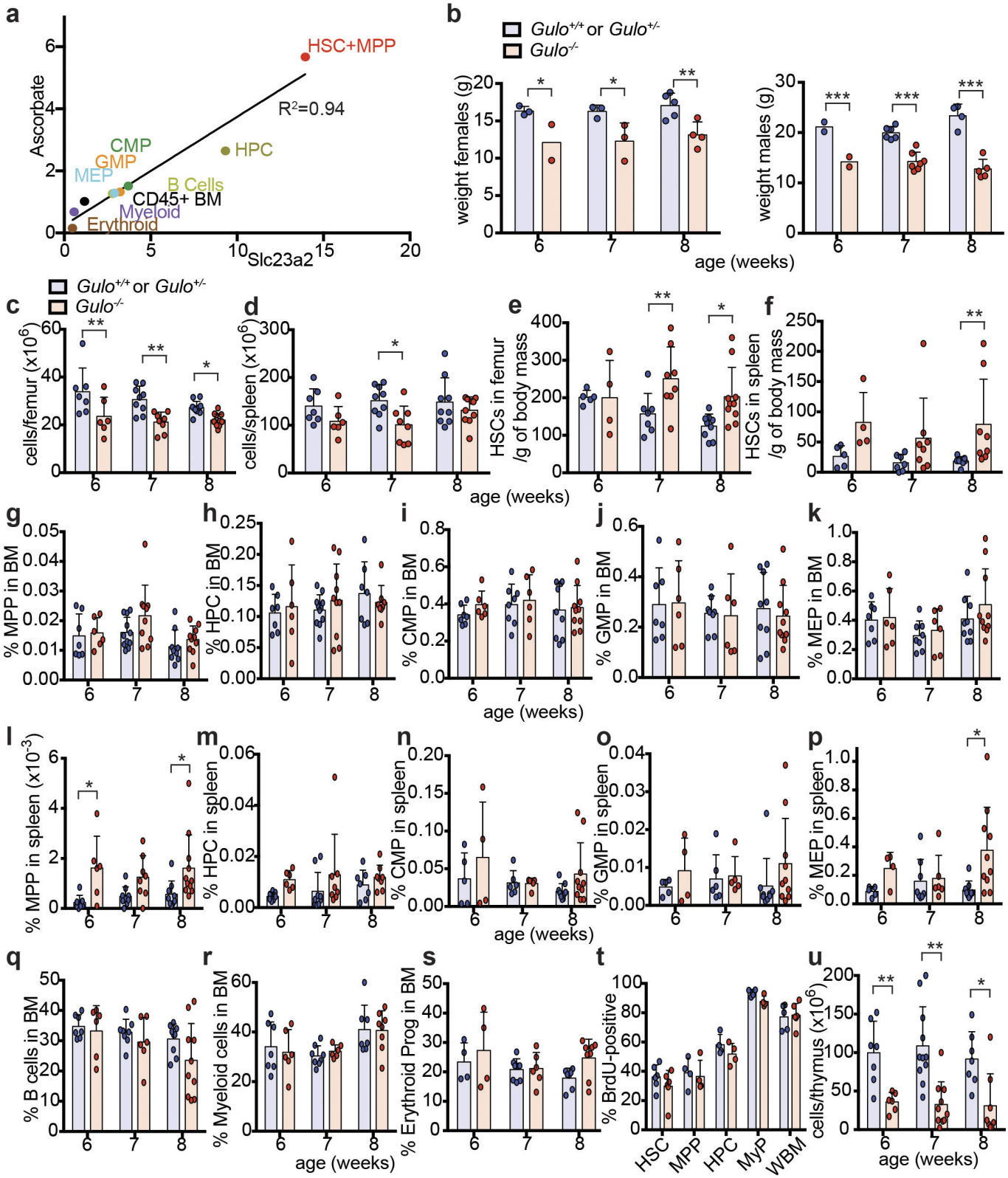

Extended Data Figure 3 | The ascorbate content in haematopoietic stem and progenitor cells correlates with ascorbate transporter expression level and the phenotype of ascorbate-depleted *Gulo*$^{-/-}$ mice. **a**, Ascorbate content versus *slc23a2* expression in haematopoietic stem and progenitor cell populations. The plotted data are from Fig. 1c, d. **b–s, u**, Analysis of ascorbate-depleted *Gulo*$^{-/-}$ mice and littermate controls (a total of $n = 5$–11 mice per genotype per time point were analysed from 3–6 independent experiments per time point). **t**, The percentage of cells that incorporated a three-day pulse of 5-bromodeoxyuridine (BrdU) at 7–8 weeks of age (a total of $n = 4$–6 mice per genotype from three independent experiments). Statistical significance was assessed with a two-way ANOVA followed by Fisher's LSD tests (**b–l**) or Mann–Whitney *U*-tests (**p**, **u**). We corrected for multiple comparisons by controlling the false discovery rate. $^{*}P < 0.05$, $^{**}P < 0.01$, $^{***}P < 0.001$. All data represent mean ± s.d.

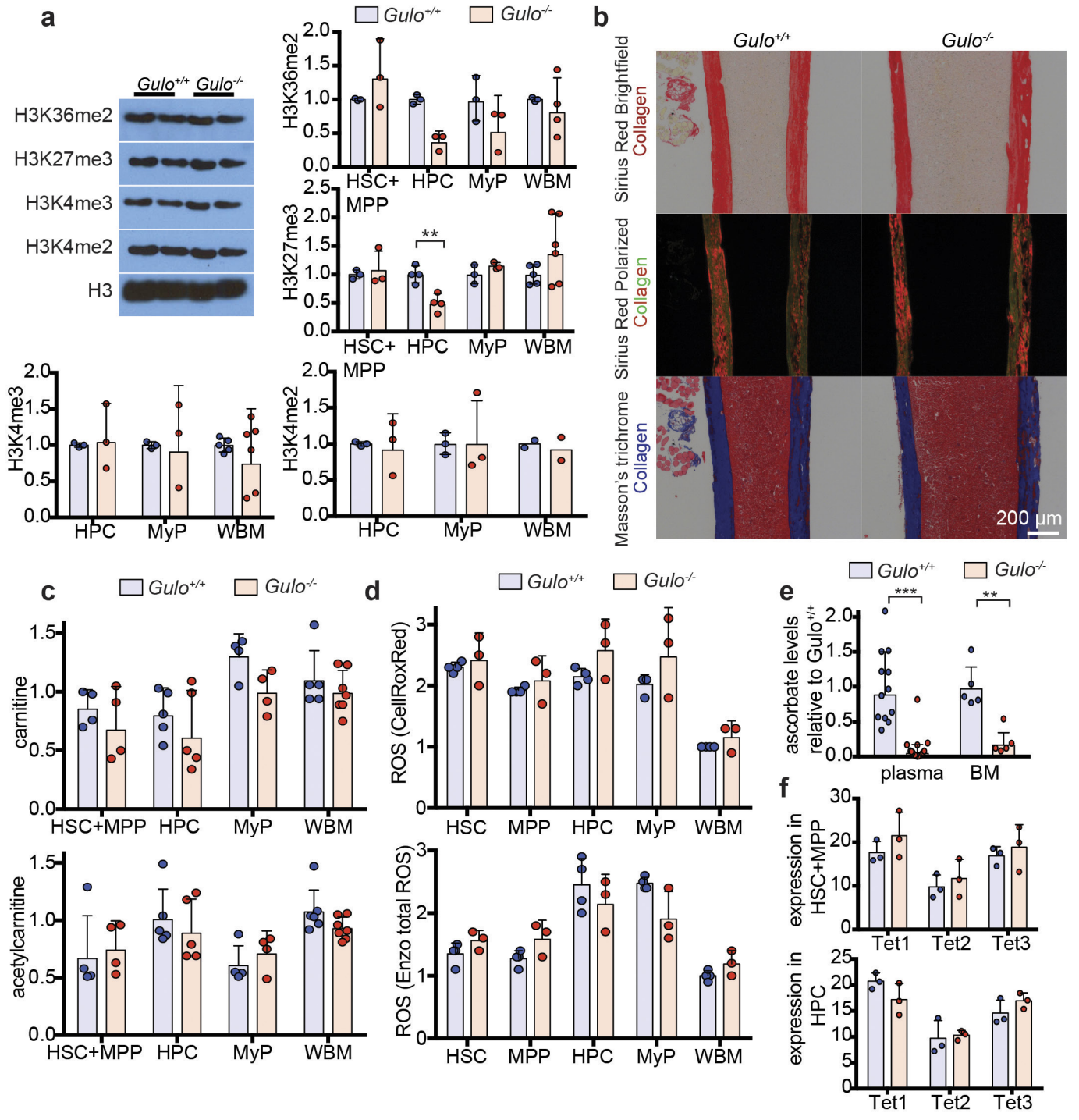

Extended Data Figure 4 | See next page for caption.

Extended Data Figure 4 | Ascorbate depletion did not have any detectable effects on global histone methylation, collagen levels, ROS levels, carnitine metabolism or Tet1–Tet3 expression in HSCs or other haematopoietic progenitors. a, Western blots with antibodies against the indicated histone modifications were performed using haematopoietic cells from eight-week-old ascorbate-depleted *Gulo*$^{-/-}$ mice and littermate controls (a total of $n = 3$–6 mice per genotype from three independent experiments). Bar graphs show band intensity relative to the band intensity of the wild-type sample of each cell type. We did not observe an increase in histone methylation for any of the modifications, as would be expected if ascorbate was promoting global histone demethylase activity. We observed reduced H3K27me3 in HPCs (note that the data in Fig. 3e show that the effects of ascorbate depletion on *Flt3*^{ITD}-driven myelopoiesis were mediated mainly by reduced Tet2 function). For gel source data, see Supplementary Fig. 1. MyP, myeloid progenitor; WBM, whole bone marrow. **b**, Histochemical staining of collagen with Sirius red (bright field or polarized light) or Masson's trichrome (blue) of bone sections from 8–16-week-old *Gulo*$^{-/-}$ mice and littermate controls (photographs are representative of 6–8 mice per genotype from two independent experiments). **c**, Carnitine and acetylcarnitine levels were measured by LC–MS/MS for the indicated cell populations obtained from 7–8-week-old *Gulo*$^{-/-}$ and littermate-control mice (a total of $n = 4$–7 mice per genotype from four independent experiments). Data show carnitine/acetylcarnitine levels relative to the average levels in wild-type whole bone marrow samples. **d**, ROS levels were measured in 12-week-old *Gulo*$^{-/-}$ and littermate-control mice using CellRox Deep Red and Enzo Total ROS dyes (a total of $n = 3$–4 mice per genotype from three independent experiments). Data show ROS levels relative to wild-type whole bone marrow samples. **e**, Ascorbate levels were measured in the plasma and bone marrow (BM) of 4–6-month-old Gulo$^{-/-}$ mice or controls (a total of $n = 12$–17 mice per genotype for plasma and $n = 5$ mice per genotype for bone marrow were analysed from three independent experiments). **f**, *Tet1–Tet3* transcript levels did not change in *Gulo*$^{-/-}$ versus littermate control mice, suggesting that the effect of ascorbate depletion on Tet activity was not due to reduced *Tet1–Tet3* transcription ($n = 3$ mice). Statistical significance was assessed with two-way ANOVAs (**a-d, f**) followed by Fisher's LSD tests or Welch's tests (**e**), or Mann–Whitney test (**a**- H3K36me2-HPC). We corrected for multiple comparisons by controlling the false discovery rate. All data represent mean ± s.d.

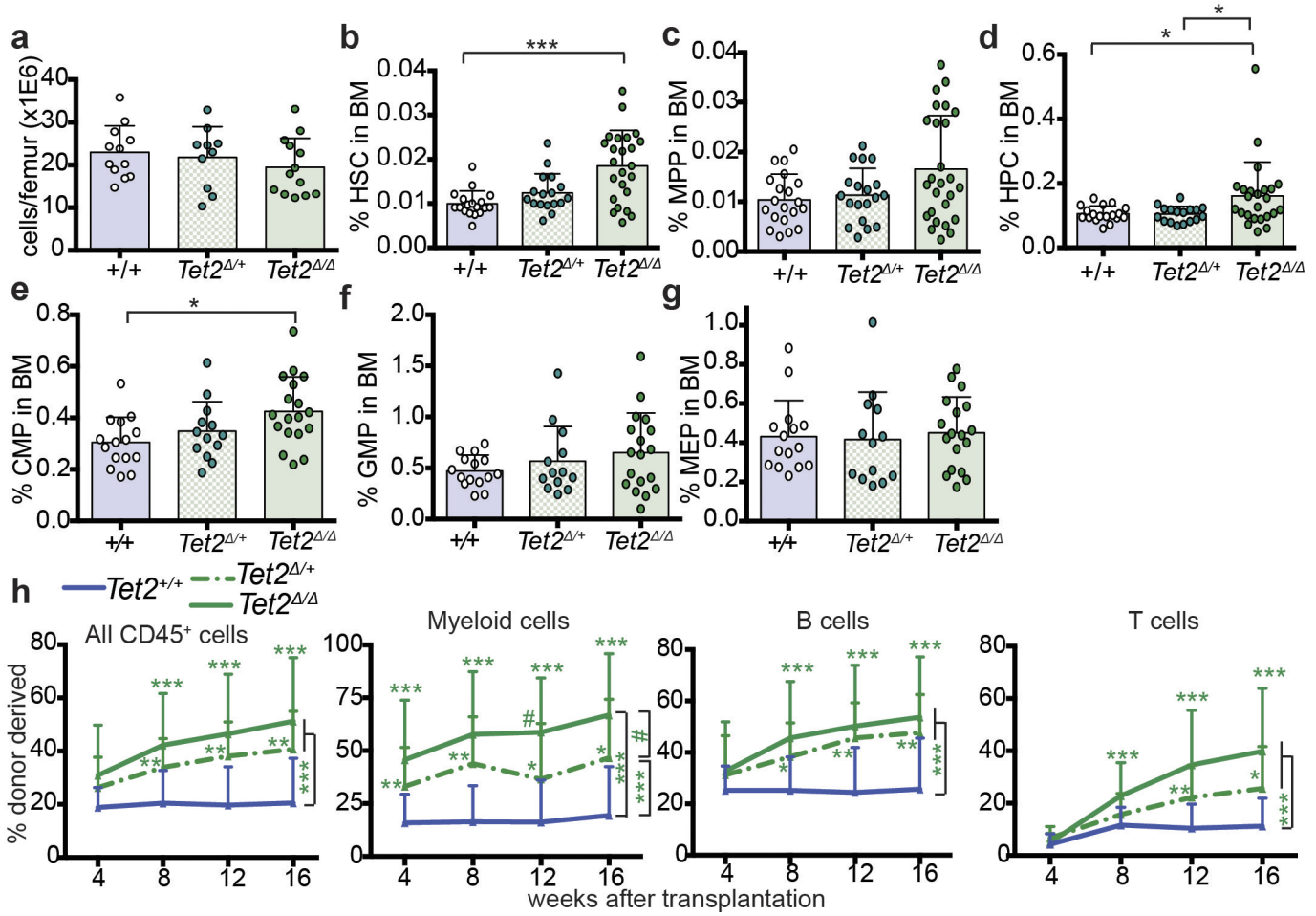

Extended Data Figure 5 | *Tet2* deletion increases HSC frequency and function. a–g, *Mx1-Cre;Tet2*$^{fl/fl}$ mice and littermate controls (+/+) were injected with poly(I:C) at 6–8 weeks of age. The frequencies of HSCs and other haematopoietic progenitors were analysed three weeks later (a total of $n = 10$–24 mice per genotype from 9–14 independent experiments). **h**, Percentage of donor-derived haematopoietic cells after competitive transplantation of 200,000 donor *Tet2*$^{+/+}$, or *Tet2*$^{\Delta/+}$ or *Tet2*$^{\Delta/\Delta}$ bone marrow cells along with 500,000 wild-type recipient competitor cells in irradiated recipient mice (a total of five donors and 15–25 recipients per treatment from five independent experiments). All data represent mean ± s.d. Statistical significance was assessed with Kruskal–Wallis tests (**a–g**), or a non-parametric mixed model followed by a Kruskal–Wallis test for individual time points (**h**). We corrected for multiple comparisons by controlling the false discovery rate. *$P < 0.05$, **$P < 0.01$, ***$P < 0.001$.

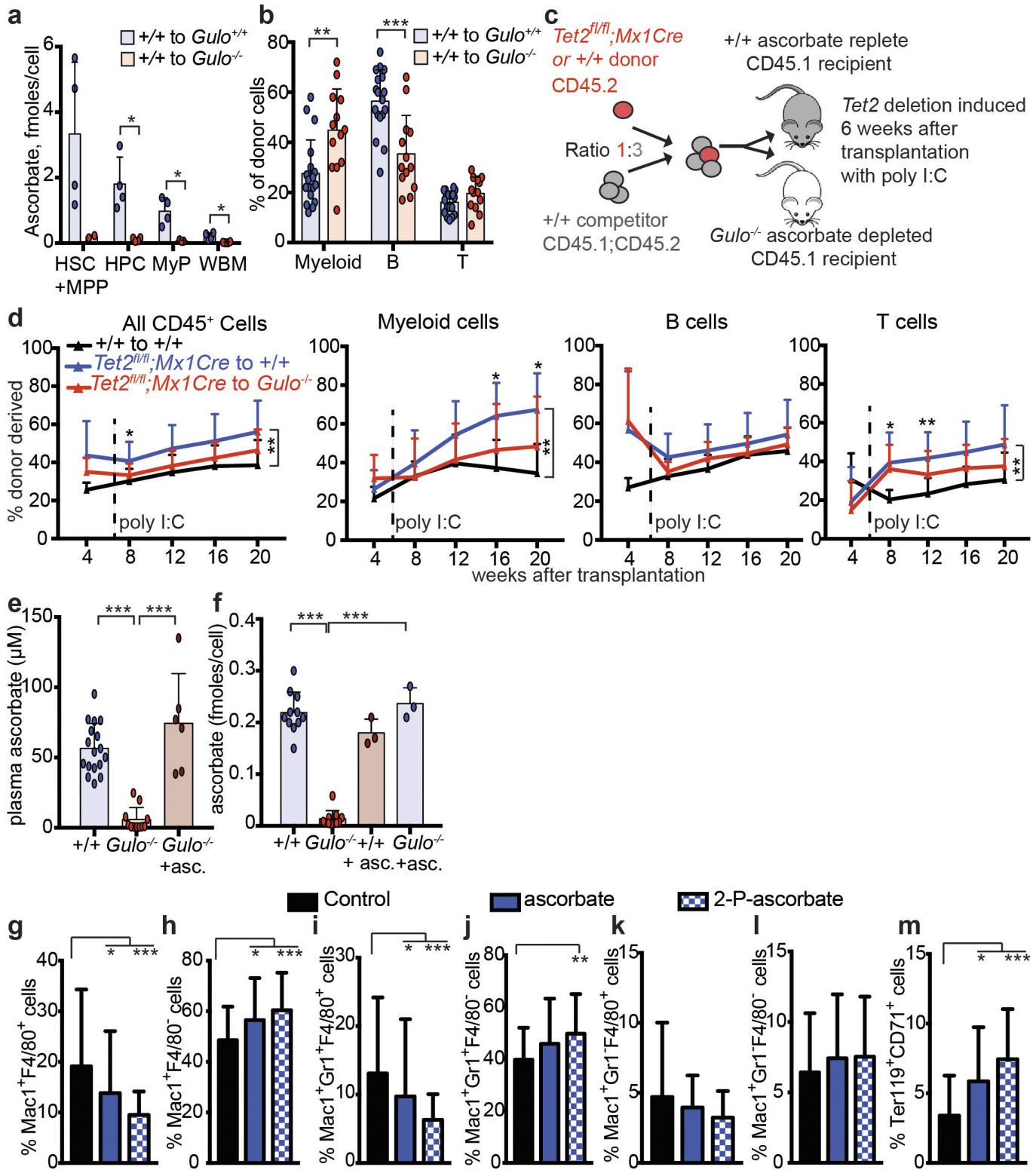

Extended Data Figure 6 | See next page for caption.

Extended Data Figure 6 | Ascorbate regulates HSC function *in vivo* and HSC differentiation in culture. a, Ascorbate levels in sorted cell populations from transplanted recipient mice (a total of $n = 2$–4 mice per genotype from two independent experiments). **b**, Percentage of donor cells that are myeloid, B or T cells in wild-type or *Gulo*$^{-/-}$ recipients 16 weeks after transplantation (a total of $n = 13$–18 mice per condition were analysed from four independent experiments). **c**, **d**, Competitive transplantation of 500,000 donor bone marrow cells from *Tet2*$^{fl/fl}$;*Mx1-cre* mice or littermate controls along with 1,500,000 competitor wild-type cells in irradiated wild-type (ascorbate-replete) or *Gulo*$^{-/-}$ (ascorbate-depleted) mice (a total of two donor mice and 5–10 recipient mice per treatment from two independent experiments). **e**, Plasma ascorbate levels in wild-type mice, *Gulo*$^{-/-}$ mice or *Gulo*$^{-/-}$ mice fed an ascorbate-supplemented diet (a total of $n = 6$–17 mice per condition were analysed from four independent experiments). **f**, Ascorbate content in bone marrow cells from wild-type and *Gulo*$^{-/-}$ mice fed normal mouse chow or an ascorbate-supplemented diet (a total of $n = 3$–11 mice per condition were analysed from three independent experiments). **g**–**m**, Myeloid and erythroid differentiation were assessed eight days after culturing HSCs in the presence or absence of ascorbate or its more stable derivative, 2-phospho-ascorbate (a total of $n = 48$ wells for myeloid and 24 wells for erythroid differentiation from two independent experiments). All data represent mean ± s.d. Statistical significance was assessed with Welch's tests (**a**, **b**), Kruskal–Wallis tests (**e**–**m**), or a non-parametric mixed model followed by a Kruskal–Wallis test for individual time points (**d**). We corrected for multiple comparisons by controlling the false discovery rate. $^{*}P < 0.05$, $^{**}P < 0.01$, $^{***}P < 0.001$.

a

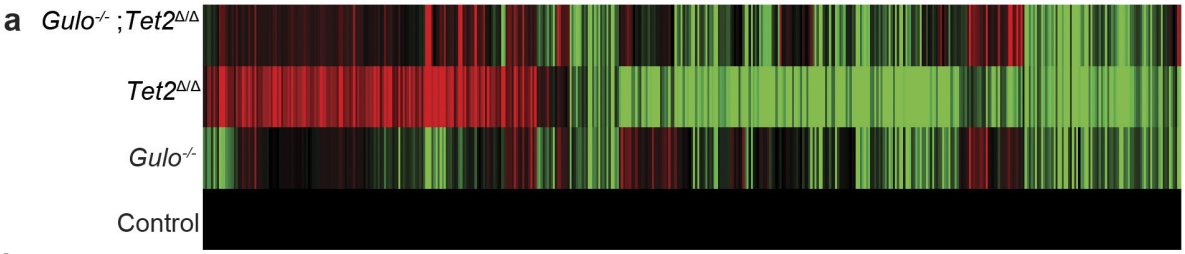

b

Gene name		Fold change relative to control (log_2)		
		Gulo$^{-/-}$	*Tet2*$^{\Delta/\Delta}$	*Gulo*$^{-/-}$;*Tet2*$^{\Delta/\Delta}$
Haematopoietic system development and function				
Gata1	GATA binding protein 1	-1.8	-3.4	-1.6
Vnn1	vanin 1	-3.4	-3.5	-3.2
Itgam	integrin alpha M	-1.4	-2.3	-2.3
Itgb2	integrin beta 2	-1.2	-2.4	-2.0
Bax	BCL2-associated X protein	-1.0	-2.7	-0.8
Nr4a1	nuclear receptor subfamily 4, group A, member 1	1.6	4.9	2.3
Cell division and DNA metabolism				
Dntt	deoxynucleotidyltransferase, terminal	-4.9	-5.7	-2.8
Hist1h2ag	histone cluster 1, H2ag	-2.2	-2.0	-2.4
Nuf2	NUF2, NDC80 kinetochore complex component	-1.2	-1.2	-1.3
Aspm	asp (abnormal spindle)-like, microcephaly associated	-1.0	-1.7	-1.0
Hist1h4a	histone cluster 1, H4a	-0.9	-1.9	-1.9
Ect2	ect2 oncogene	-0.9	-2.1	-1.7
Hist1h2ak	histone cluster 1, H2ak	-0.8	-0.8	-0.7
Cenpw	centromere protein W	-0.8	-3.5	-3.0
Tpx2	TPX2, microtubule-associated protein homolog	-0.7	-1.5	-0.6
Ccdc69	coiled-coil domain containing 69	1.1	1.6	1.4
Signalling				
Ndrg2	N-myc downstream regulated gene 2	-1.8	-0.9	-1.1
Sh3d19	SH3 domain protein D19	-1.8	-6.9	-2.2
Igf1	insulin-like growth factor 1	-1.2	-0.8	-3.4
Pdgfrb	platelet derived growth factor receptor, beta	0.9	1.4	1.4
Robo3	roundabout homolog 3	1.8	3.9	1.8
Metabolism				
Acy3	aspartoacylase 3	-2.0	-2.5	-0.7
Gpt2	glutamic pyruvate transaminase 2	-1.3	-2.9	-1.2
Gatm	glycine amidinotransferase	-0.9	-1.2	-0.9
Unknown function				
Tpm3-rs7	tropomyosin 3, related sequence 7	-4.6	-5.4	-5.8
Mtx3	metaxin 3	0.7	2.9	1.1
Fam102b	family with sequence similarity 102, member B	1.2	1.2	0.8

c

Downregulated gene sets	Rank among most downregulated gene sets	
	Gulo$^{-/-}$ *vs* Control	*Tet2*$^{\Delta/\Delta}$ *vs* Control
Antimicrobial peptides	#1	#2
Myeloid mediated immunity	#6	#17
Activation of matrix metalloproteinases	#12	#1
Basement membranes	#14	#13

Extended Data Figure 7 | Gene expression changes in HSCs/MPPs from *Gulo*$^{-/-}$, *Tet2*$^{\Delta/\Delta}$ and *Tet2*$^{\Delta/\Delta}$;*Gulo*$^{-/-}$ mice relative to control HSCs/MPPs. a–c, HSCs/MPPs were isolated from 4–5-month-old mice of the indicated genotypes. Mice from all treatments were maintained on low ascorbate water and treated with poly(I:C) to induce *Tet2* deletion by Mx1-Cre two months before HSC/MPP isolation. **a**, Fold-change values for all genes that significantly differed among any combination of genotypes (DESeq2 likelihood ratio tests for differential expression, corrected for multiple comparisons by controlling the false discovery rate). The value for each gene in the control cells was set to one. Red and green indicate increases and decreases in gene expression, respectively. The number of genes in *Gulo*$^{-/-}$ and *Tet2*$^{\Delta/\Delta}$ HSCs/MPPs that changed in expression in the same direction in both genotypes relative to control HSCs/MPPs was significantly higher than would be expected by chance ($P = 0.01$, binomial test). **b**, Fold change (log_2) for HSCs/MPPs of each genotype relative to control HSCs/MPPs. All genes that changed in the same direction in all three genotypes relative to control are shown and for which the log_2 fold change was >0.7 or <-0.7 and fragments per kilobase of transcript per million mapped reads (FPKM) >1. Negative fold change values indicate that the expression of the indicated gene decreased in the indicated genotypes compared to control and positive values indicate that the expression of the gene increased. **c**, Gene set enrichment analysis showed that of the top 20 gene sets (based on normalized enrichment score) that were downregulated in *Gulo*$^{-/-}$ compared to control HSCs/MPPs, 4 were also among the top 20 gene sets downregulated in *Tet2*$^{\Delta/\Delta}$ compared to control HSCs/MPPs ($n = 3$ mice per genotype, except for the *Tet2*$^{\Delta/\Delta}$ treatment, for which $n = 2$).

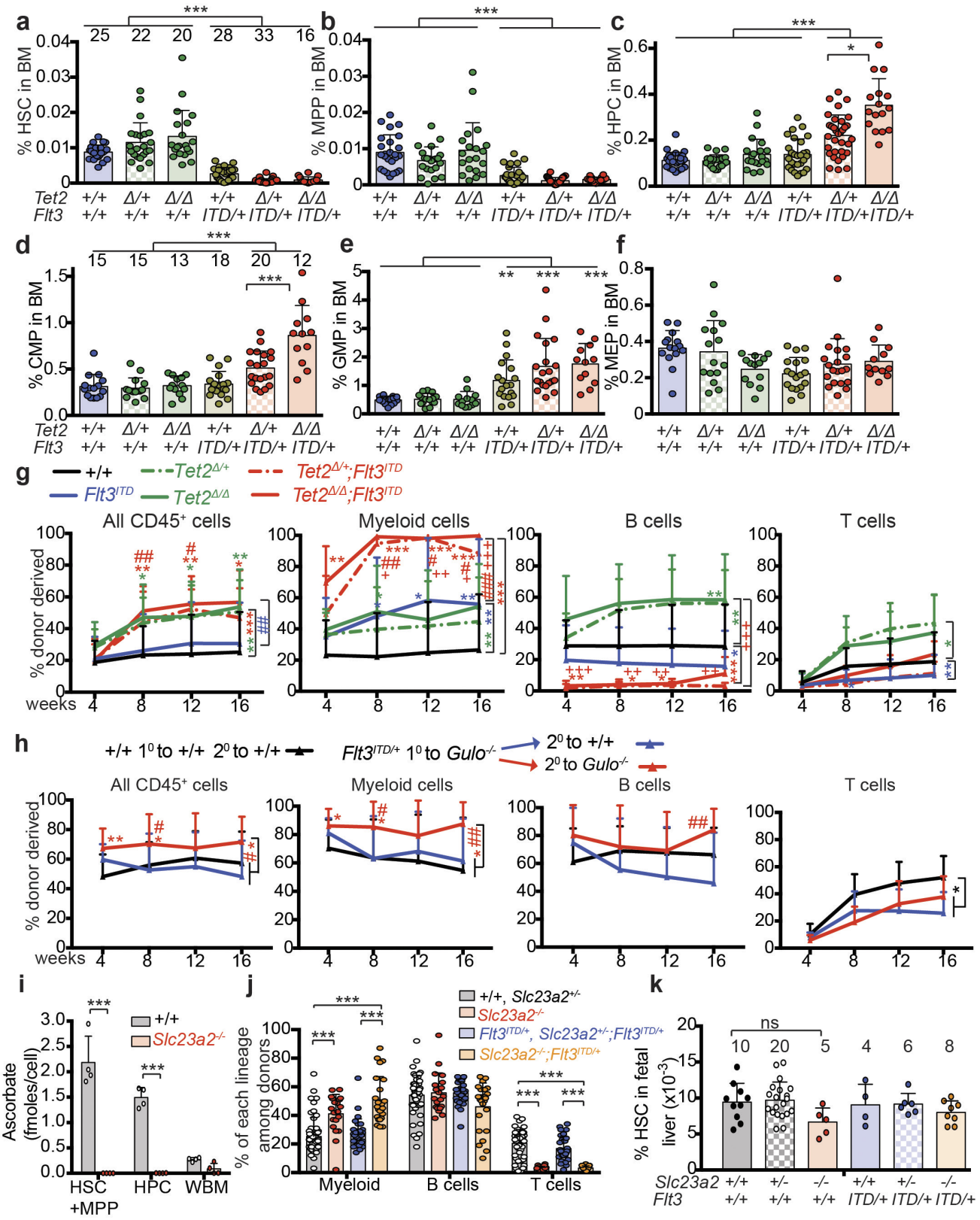

Extended Data Figure 8 | See next page for caption.

Extended Data Figure 8 | Collaboration between *Flt3*^{ITD} and either *Tet2* deficiency or ascorbate depletion. **a**–**f**, Analysis of the frequencies of haematopoietic stem and progenitor cell populations in the bone marrow of 10–12-week-old *Mx1-Cre;Tet2*$^{fl/fl}$*;Flt3*^{ITD} mice and littermate controls three weeks after poly(I:C) treatment (12–17 independent experiments; the numbers of mice per treatment in **a**–**c** are shown across the top of **a** and for **d**–**f** across the top of **d**). **g**, Percentage of donor-derived haematopoietic cells after competitive transplantation of 300,000 donor bone marrow cells of the indicated genotypes along with 300,000 competing recipient cells in irradiated recipient mice (a total of 2–5 donor mice and 6–20 recipient mice per treatment from five independent experiments). **h**, Secondary transplantation of 5 million bone marrow cells from primary *Gulo*$^{-/-}$ (ascorbate-depleted) recipients of *Flt3*$^{ITD/+}$ cells in irradiated wild-type or ascorbate-depleted *Gulo*$^{-/-}$ recipient mice (a total of three donor mice and 10–18 recipient mice per treatment from three independent experiments). *Comparison to wild type and #comparison to *Flt3*$^{ITD/+}$. **i**, Ascorbate levels in donor cells of the indicated genotypes sorted from transplant recipients (a total of $n = 4$ mice per condition from 2 independent experiments). 1°, primary transplantation; 2°, secondary transplantation. **j**, Frequencies of donor cells of the indicated genotypes in the blood of transplant recipients described in Fig. 3f, g. **k**, Analysis of HSC frequency in the fetal liver of embryonic day (E)17.5 mice of the indicated genotypes (five independent experiments; the numbers of mice per treatment are shown across the top). All data represent mean ± s.d. Statistical significance was assessed with one-way ANOVAs followed by Fisher's LSD tests (**d**, **k**) or Kruskal–Wallis tests (**a**–**c**, **e**). In other cases, we used two-way ANOVAs followed by Fisher's LSD tests (**i**), Kruskal–Wallis tests (**j**) or a non-parametric mixed model followed by Kruskal–Wallis tests for individual time points (**g**, **h**). We corrected for multiple comparisons by controlling the false discovery rate. *$P < 0.05$, **$P < 0.01$, ***$P < 0.001$; #$P < 0.05$, ##$P < 0.01$, ###$P < 0.001$; +$P < 0.05$, ++$P < 0.01$, +++$P < 0.001$. *Comparison to the wild-type (+/+) condition, #comparison to the *Flt3*^{ITD} condition and +comparison to the *Tet2*$^{\Delta/+}$ or *Tet2*$^{\Delta/\Delta}$ conditions. To simplify the representation of statistical significance in **g**, statistical significance was only noted when both *Tet2*$^{\Delta/+}$ and *Tet2*$^{\Delta/\Delta}$ conditions, or both *Tet2*$^{\Delta/+}$*;Flt3*^{ITD} and *Tet2*$^{\Delta/\Delta}$*;Flt3*^{ITD} conditions, were significantly different from other conditions).

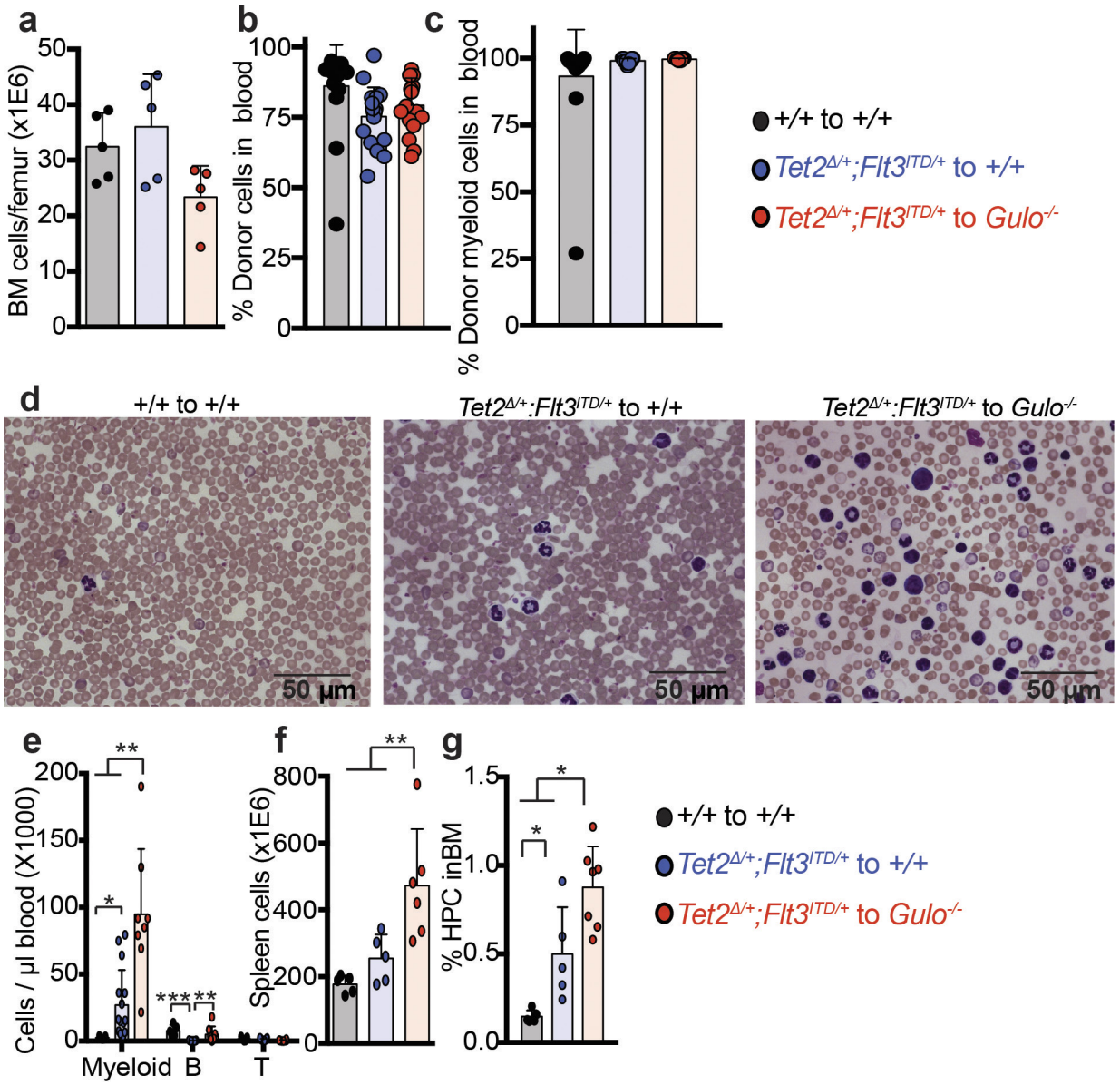

Extended Data Figure 9 | Analysis of *Tet2*$^{\Delta/+}$;*Flt3*^{ITD} leukaemias. **a**–**g**, Analysis of recipient mice described in Fig. 4a–d. Statistical significance was assessed with one-way ANOVAs followed by Fisher's LSD tests (**f**, **g**) or Kruskal–Wallis tests (**e**). **d**, Representative images from the experiments quantified in Fig. 4a. All data represent mean ± s.d. We corrected for multiple comparisons by controlling the false discovery rate. $*P < 0.05$, $**P < 0.01$, $***P < 0.001$.

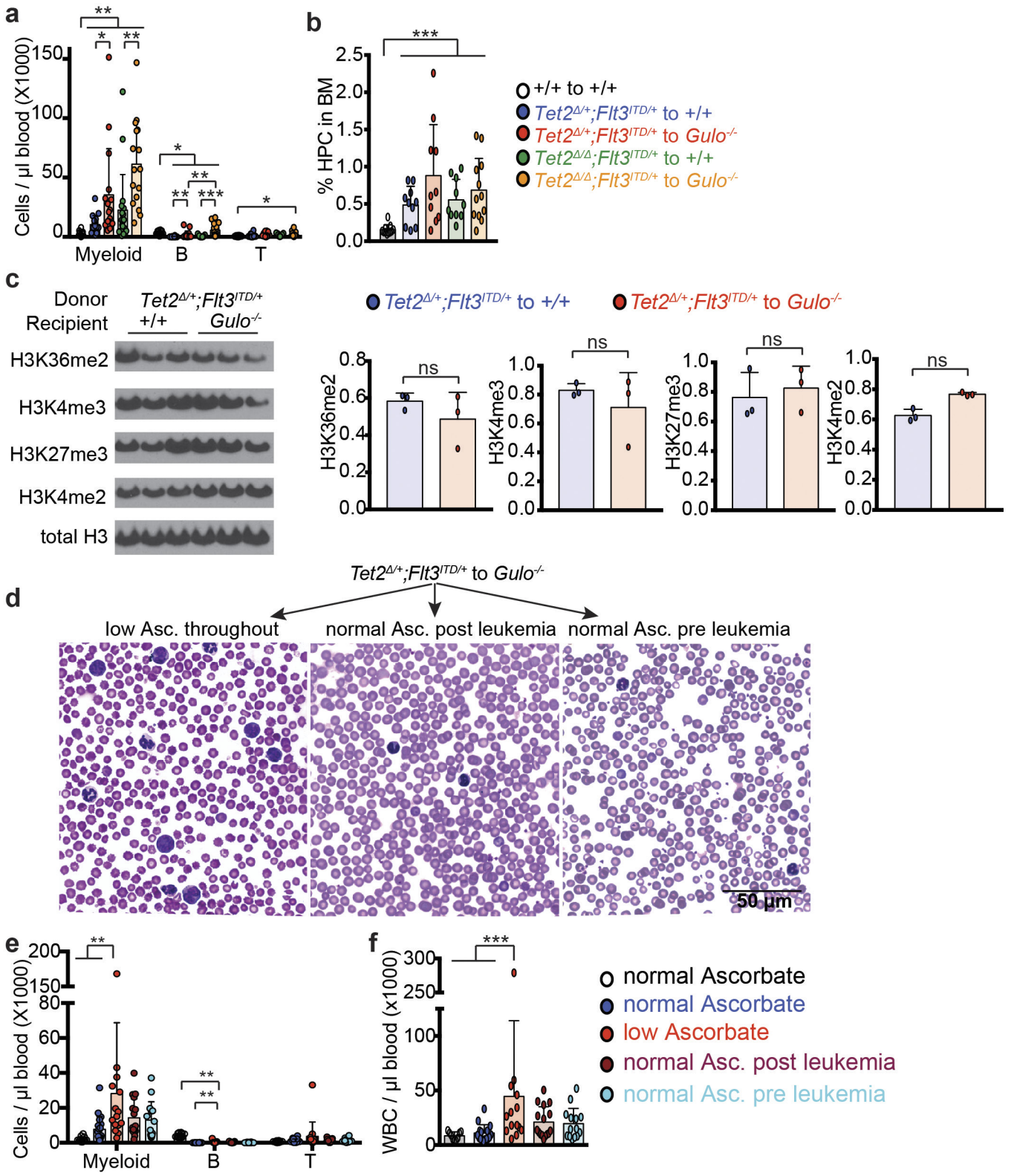

Extended Data Figure 10 | Analysis of *Tet2*$^{\Delta/+}$;*Flt3*^{ITD} and *Tet2*$^{\Delta/\Delta}$;*Flt3*^{ITD} leukaemias. a, **b**, Analysis of recipient mice described in Fig. 4e–j. Statistical significance was assessed with one-way ANOVAs followed by Fisher's LSD tests (**b**) or Kruskal–Wallis tests (**a**). **c**, Western blots with antibodies against the indicated histone modifications were performed using protein extracted from *Tet2*$^{\Delta/+}$;*Flt3*$^{ITD/+}$ leukaemia cells isolated by flow cytometry from wild-type or ascorbate-depleted *Gulo*$^{-/-}$ transplant recipients (results are representative of two independent experiments). **d**, Diff-Quik-stained blood smears from *Gulo*$^{-/-}$ recipients of *Tet2*$^{\Delta/+}$;*Flt3*$^{ITD/+}$ cells fed with an ascorbate-supplemented diet before and after the engraftment of leukaemia cells (representative images from the experiments described in Fig. 5a and quantified in Fig. 5c). Cells with an immature blast-like morphology were more abundant in the blood of ascorbate-depleted *Gulo*$^{-/-}$ recipients compared to ascorbate-fed *Gulo*$^{-/-}$ recipients. **e**, **f**, WBCs in recipient mice from the experiment described in Fig. 5a. The statistical significance of differences among treatments was assessed with Kruskal–Wallis tests (**a**, **e**, **f**) or a one-way ANOVA (**b**) or a two-way ANOVA followed by Fisher's LSD tests (**c**). All data represent mean ± s.d. We corrected for multiple comparisons by controlling the false discovery rate. *$P < 0.05$, **$P < 0.01$, ***$P < 0.001$.

nature research

Corresponding author(s): Sean J. Morrison

☐ Initial submission ☐ Revised version ☒ Final submission

Life Sciences Reporting Summary

Nature Research wishes to improve the reproducibility of the work that we publish. This form is intended for publication with all accepted life science papers and provides structure for consistency and transparency in reporting. Every life science submission will use this form; some list items might not apply to an individual manuscript, but all fields must be completed for clarity.

For further information on the points included in this form, see Reporting Life Sciences Research. For further information on Nature Research policies, including our data availability policy, see Authors & Referees and the Editorial Policy Checklist.

Experimental design

1. Sample size

Describe how sample size was determined.

The sample size used in each experiment was not predetermined or formally justified for statistical power. For samples with low variation, for example metabolite levels in HSCs, generally 4-6 samples per condition were analysed in each experiment. For samples with large variation, for example transplantation experiments, generally 10-20 samples per condition were analysed in each experiment.

2. Data exclusions

Describe any data exclusions.

In Figure 5f, data from 1 human patient was excluded due to clinical evidence of myelodysplastic syndrome. In Figures 3e and ED Figure 8g, some recipient mice were excluded because they showed no reconstitution, suggesting no HSCs were present among the donor cells, therefore those samples provided no information on HSC activity. In ED Figure 6d, time point 4 was excluded from the statistical analysis because it involved comparisons between genotypes before Tet2 conditional deletion.

3. Replication

Describe whether the experimental findings were reliably reproduced.

The experimental findings were reproduced in multiple independent experiments. The number of independent experiments and biological replicates in each data panel is indicated in the figure legends. Data shown in the figures represent the aggregate of all independent experiments in almost all cases. Data shown in a minority of panels are from a representative experiment (e.g. western blots) and in those cases the number of independent experiments that reproduced the finding is also indicated in the figure legends.

4. Randomization

Describe how samples/organisms/participants were allocated into experimental groups.

No formal randomization techniques were used, however, samples were allocated randomly into experimental groups and processed in an arbitrary order.

5. Blinding

Describe whether the investigators were blinded to group allocation during data collection and/or analysis.

The investigators were not blinded to group allocation during data collection and analysis

Note: all studies involving animals and/or human research participants must disclose whether blinding and randomization were used.

6. Statistical parameters

For all figures and tables that use statistical methods, confirm that the following items are present in relevant figure legends (or in the Methods section if additional space is needed).

n/a	Confirmed
☐	☒ The exact sample size (*n*) for each experimental group/condition, given as a discrete number and unit of measurement (animals, litters, cultures, etc.)
☐	☒ A description of how samples were collected, noting whether measurements were taken from distinct samples or whether the same sample was measured repeatedly
☐	☒ A statement indicating how many times each experiment was replicated
☐	☒ The statistical test(s) used and whether they are one- or two-sided (note: only common tests should be described solely by name; more complex techniques should be described in the Methods section)
☐	☒ A description of any assumptions or corrections, such as an adjustment for multiple comparisons
☒	☐ The test results (e.g. *P* values) given as exact values whenever possible and with confidence intervals noted
☐	☒ A clear description of statistics including central tendency (e.g. median, mean) and variation (e.g. standard deviation, interquartile range)
☐	☒ Clearly defined error bars

See the web collection on statistics for biologists for further resources and guidance.

Software

Policy information about availability of computer code

7. Software

Describe the software used to analyze the data in this study.

GraphPad Prism v7.0 and R 3.2.1 were used for all statistical tests. RNA-seq analysis was performed using FastQC 0.11.2 (raw reads quality checking), Trimmomatic 0.32 (raw reads quality filtering), TopHat 2.0.12 with Bowtie2 2.2.3 (reads mapping), SAMtools 0.1.19 (mapped reads quality filtering), HTSeq 0.6.1 (mapped read counts quantification), DESeq2 1.8.2 and RUVSeq 1.2.0 with R 3.2.1 (differential expression), and Cluster 3.0 (clustering and heatmap generation). Multiquant, MetaboAnalyst and Simca were used to analyze metabolomics data.

For manuscripts utilizing custom algorithms or software that are central to the paper but not yet described in the published literature, software must be made available to editors and reviewers upon request. We strongly encourage code deposition in a community repository (e.g. GitHub). *Nature Methods* guidance for providing algorithms and software for publication provides further information on this topic.

Materials and reagents

Policy information about availability of materials

8. Materials availability

Indicate whether there are restrictions on availability of unique materials or if these materials are only available for distribution by a for-profit company.

There are no restrictions on the availability of materials. No unique materials were used in this study. Antibodies and chemical reagents were purchased from for-profit companies as detailed in the methods.

9. Antibodies

Describe the antibodies used and how they were validated for use in the system under study (i.e. assay and species).

Please see attached list of antibodies, clone names, suppliers, catalogue numbers and lot numbers. Please see statement and citations on suppliers' websites regarding antibody specificity. Antibodies used to purify haematopoietic stem cells have been thoroughly validated in previous publications by this laboratory (e.g. Cell 121:1109, Blood 107:924, Nature 526:126).

10. Eukaryotic cell lines

a. State the source of each eukaryotic cell line used.

No cell lines were used

b. Describe the method of cell line authentication used.

No cell lines were used

c. Report whether the cell lines were tested for mycoplasma contamination.

No cell lines were used

d. If any of the cell lines used are listed in the database of commonly misidentified cell lines maintained by ICLAC, provide a scientific rationale for their use.

No cell lines were used

Animals and human research participants

Policy information about studies involving animals; when reporting animal research, follow the ARRIVE guidelines

11. Description of research animals

Provide details on animals and/or animal-derived materials used in the study.

C57BL/6 mice were used. Details and references for each mutant strain are described in the methods section. Both male and female mice were used for most experiments unless otherwise specified. 2-6 month old animals were used for most experiments as specified in the text.

Policy information about studies involving human research participants

12. Description of human research participants

Describe the covariate-relevant population characteristics of the human research participants.

Bone marrow aspirates were collected from male and female patients, aged 34-85, who were being assessed for lymphoma. Experiments in Figure 5f-g were performed using aspirates in which there was no evidence of lymphoma or myelodysplastic syndrome was observed. Age and sex of the patients were shared with us. We did not obtain additional demographic data on the patients who donated the samples because per our IRB approval, the samples were de-identified before being shared with us.

nature research

Corresponding author(s): Sean J. Morrison

☐ Initial submission ☐ Revised version ☒ Final submission

Flow Cytometry Reporting Summary

Form fields will expand as needed. Please do not leave fields blank.

Data presentation

For all flow cytometry data, confirm that:

☒ 1. The axis labels state the marker and fluorochrome used (e.g. CD4-FITC).

☒ 2. The axis scales are clearly visible. Include numbers along axes only for bottom left plot of group (a 'group' is an analysis of identical markers).

☒ 3. All plots are contour plots with outliers or pseudocolor plots.

☒ 4. A numerical value for number of cells or percentage (with statistics) is provided.

Methodological details

5. Describe the sample preparation.	Bone marrow cells were obtained by flushing femurs and tibias with a 25G needle or by crushing femurs, tibias, vertebrae, and pelvic bones with a mortar and pestle, in Ca2+ and Mg2+ free Hank's buffered salt solution (HBSS; Gibco), supplemented with 2% heat-inactivated bovine serum (HIBS, Gibco). Spleens and thymuses were dissociated by crushing followed by gentle trituration. All cell suspensions were filtered through a 40 µm cell strainer. For flow cytometric analysis and isolation, cells were incubated with combinations of fluorescent antibodies to cell-surface markers. Antibody staining was generally performed at 4°C for 30 minutes. For isolation of all c-kit+ cell populations, cells were pre-enriched before flow cytometry using paramagnetic microbeads and an autoMACS magnetic separator (Miltenyi Biotec).
6. Identify the instrument used for data collection.	BD FACS Aria II or FACS Aria Fusion (for cell sorting or analysis), BD Canto (for analysis).
7. Describe the software used to collect and analyze the flow cytometry data.	BD FACS DiVa
8. Describe the abundance of the relevant cell populations within post-sort fractions.	The abundance of the relevant cell populations within post-sort fractions was almost 100% in pilot experiments. The abundance could not be tested after every experiment because cells were usually sorted directly in lysis buffer.
9. Describe the gating strategy used.	Please see the attached supplementary figure showing the gating strategy for haematopoietic stem and progenitor cells

Tick this box to confirm that a figure exemplifying the gating strategy is provided in the Supplementary Information. ☒